Analytical models for growth by metal organic vapor phase epitaxy. I.Isothermal models

Semicond. Sci. Technol. 5 (1990) 16–35. Printed in the UK

Analytical models for growth by metal organic vapour phase epitaxy: I. Isothermal models

W G J H M van Sark, G Janssen, M H J M de Croon and L J Giling

Department of Experimental Solid State Physics, RIM, Faculty of Science, University of Nijmegen, Toernooiveld, 6525 ED Nijmegen, The Netherlands

Received 31 March 1989, in final form 11 July 1989, accepted for publication 26 July 1989

Abstract. For a proper description of growth by metal organic vapour phase epitaxy the three-dimensional Navier–Stokes partial differential equations need to be solved which govern the following series of processes: (i) transport by diffusion and flow through the gas phase, (ii) reactions which take place in this gas phase, (iii) reactions which take place at the surface. For this paper we are at first interested in the medium- and higher-temperature regions, which cover the growth determined by diffusion through the gas phase (medium temperature) and the growth that is determined by the desorption of growth species (higher temperature). Using a number of well justified assumptions one can reduce the problem to a two-dimensional one. For the diffusion-limited region (i.e. medium-temperature region) the effect of different flow profiles (plug flow, parabolic flow, linear increasing velocity and combination of plug and linear profile) on the growth rate has been studied under isothermal conditions. It was found that all profiles yield the same growth rate within a few per cent, so that it suffices to use the simple plug flow profile in growth rate calculations. It is also shown that axial diffusion is an important effect only at the end of long reactors. Finally a model is derived in which surface reaction kinetics is combined with the diffusion-limited model for the isothermal case.

1. Introduction

Metal organic vapour phase epitaxy (MOVPE) is at present an important epitaxy technique for the growth of III–V compound semiconductor materials [1, 2]. Many electronic and optical devices after being demonstrated to work on a laboratory scale are now produced commercially on an industrial scale by MOVPE. Studies that have been performed over the past twenty years since the introduction of MOVPE by Manasevit [3] have dealt mainly with fundamental and technical aspects. Flow dynamics, reactor design and depletion effects have received to date only little attention, but interest is growing [4–9]. As flow dynamics of vapour phase epitaxy (VPE) processes are very complex, one is inclined to study these phenomena with the help of numerical simulations [6–9]. Although the graphical presentations of results obtained by these simulations are certainly instructive (e.g. the occurrence of rolls [7]) we concentrate on analytical solutions because they give more and direct insight in the physics and chemistry of the MOVPE process.

To obtain analytical solutions one has to solve the three-dimensional Navier–Stokes partial differential equations [10]. As this is next to impossible in general a number of simplifications have to be used. The assumptions from which the simplifications originate must be physically justified. Mathematical simplifications which are made solely for the purpose of obtaining differential equations that are simple to solve are not to be used as they generally lead to unrealistic situations.

The models that are derived are in principle generally applicable, however, they are derived here using observations made of the growth of (Al)GaAs [1–4, 11–15]. It is found that the temperature dependence of the growth of GaAs can be divided in three temperature regions: low, medium and high. In the low- and high-temperature regions the growth rate is strongly temperature dependent. It has been suggested that in the low-temperature region surface reactions (adsorption of As and Ga species [11]) or gas-phase reactions (pyrolysis of As and Ga species [12, 13]) are growth-rate limiting. In the high-temperature region the Ga adsorption–desorption equilibrium is considered to be growth-rate limiting [11, 14, 15]. In the medium-temperature region growth is

0268-1242/90/010016+20 $03.50

mass transport limited by the diffusion of Ga growth species towards the susceptor [1-4, 11, 14] and therefore does not show a (or only a weak) temperature dependence.

In this series of papers [16, 17] we are mainly interested in the medium- and high-temperature regions. Before the different models are treated a thorough analysis is performed on the validity of the assumptions needed to simplify the three-dimensional Navier-Stokes partial differential equations. For the diffusion-limited region (medium temperature) first the effect of different flow profiles (namely, plug flow, parabolic flow, linear increasing velocity) is studied in the isothermal case. In forthcoming papers [16, 17] a temperature gradient will be introduced and the influence of the Soret or thermodiffusion effect will be studied. For the high-temperature region, where desorption of growth species becomes important, a similar analysis will be performed. The studies lead to an analytical expression for the growth rate over the two temperature regions considered. The theoretical results are compared with experimental results for the growth of Si, GaAs and AlGaAs grown within the two temperature regions [17, 18].

2. Problem definition and assumptions

2.1. Assumptions and their justification

In this section the assumptions made to simplify the solution of the three-dimensional Navier-Stokes partial differential equations are physically justified. The analytical models will be developed for a horizontal rectangular reactor at atmospheric pressure as depicted in figure 1. The reactor is heated at the bottom and cooled at the top. A cartesian coordinate system is used, with the x coordinate in the direction of the forced gas flow, the y coordinate perpendicular to the flow direction (figure 2(*a*)) and the z coordinate in the direction of the width of the reactor (figure 2(*b*)). Heating starts at $x = 0$. The height of the reactor is h and the width is b. In the reactor a susceptor is placed on which substrates are positioned. The gas phase of such a reactor can be described by the velocity profile $v(x, y, z, t)$, the temperature profile $T(x, y, z, t)$ and the concentration profile for each $(i, i = 1, \ldots, n)$ gas-phase component $C_i(x, y, z, t)$, where t denotes the time dependence. These variables can be found by solving the three-dimensional Navier-Stokes, continuity and diffusion partial differential equations [10]. These can be simplified using a number of assumptions, which are justified keeping the growth of GaAs from trimethylgallium (TMG) and AsH_3 in mind. The formulation of the assumptions may seem extensive; however, in the past several authors were not as careful as they should have been in formulating the assumptions on which their models were based. Therefore it is not always clear whether the derived models are valid or not. In the derivation of the analytical models the following assumptions are used.

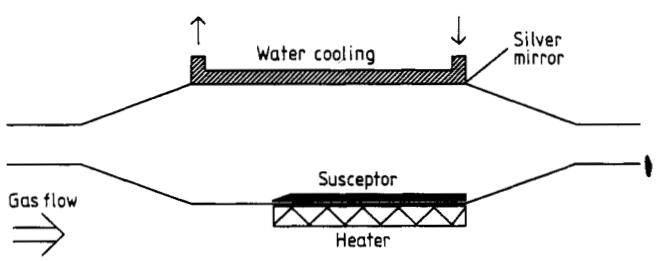

Figure 1. Schematic overview of the MOVPE reactor cell; the gas is coming from the left. The reactor is resistance heated at the bottom and water-cooled at the top.

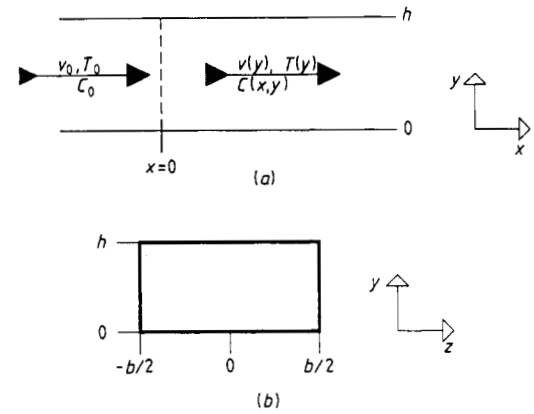

Figure 2. Definition of cartesian coordinate system: (*a*) side view; (*b*) cross section.

Assumption 1. The amounts of hydrides and metal alkyls are small (typically $< 1\%$) as compared with the amount of carrier gas (i.c. H_2). Therefore the flow dynamics are completely determined by the carrier gas. As the growth of GaAs is controlled in the diffusion-limited region by the diffusion of TMG towards the substrate only the concentration of one gas-phase component is considered. The concentration profile $C_i(x, y, z, t)$ can thus be simplified to $C(x, y, z, t)$.

Assumption 2. For all times $t \geqslant 0$ the velocity profile $v(x, y, z, t)$, temperature profile $T(x, y, z, t)$ and concentration profile $C(x, y, z, t)$ at any position (x, y, z) are independent of time, thus a (quasi) stationary situation is established.

Assumption 3. Under all conditions and for any position (x, y, z) the flow is laminar and streamlines are horizontal and thus parallel to the susceptor. Choosing the right reactor dimensions and using H_2 (or He) as carrier gas it is simple to obtain laminar, metastable flows for completely developed flow profiles [19]. When the gas is flowing from the cold zone $(x < 0)$ to the high-temperature zone $(x \geqslant 0)$ it experiences a temperature shock, which causes the gas to expand which can lead to unwanted return flows [20]. This can be prevented by using a low reactor ($\leqslant 2$ cm) and sufficiently high gas velocities (room temperature mean flow rate ~ 10 cm s^{-1}). Due to the temperature shock the flow profile has to be re-established. The streamlines seem to recover quickly from this shock (within $\simeq 1$ cm) [5]. However, the velocity and temperature profiles, which are coupled, are re-established more slowly. Entrance lengths for these

profiles have been calculated to be $x_v = 0.04\,h\,Re$ and $x_T = 0.28\,h\,Re$ [19], where x_v and x_T are the entrance lengths for the velocity and temperature profile respectively, Re is the Reynolds number and h the height of the reactor. This means that the temperature profile determines the dimensions of the entrance region.

Assumption 4. At the entrance of the reactor, up to $x = 0$, the flow is laminar with an average velocity $\bar{v}$ and input concentration of the group III component C_0. Hence for all $x < 0$ the velocity profile $v(x, y, z, t)$ is independent of x, whereas the temperature profile $T(x, y, z, t)$ and concentration profile $C(x, y, z, t)$ are independent of (x, y, z).

Assumption 5. As we are not interested in the development of the flow but in already fully developed flow profiles, it is assumed that no entrance region exists in which the profiles develop. Alternatively, one can assume that the entrance lengths of the velocity and temperature profiles are reduced to an infinitesimal size. Hence for all $x \geqslant 0$ the velocity profile $v(x, y, z, t)$ and temperature profile $T(x, y, z, t)$ are independent of x. These profiles are thus fully developed, which does not hold for the concentration profile $C(x, y, z, t)$.

Assumption 6. The transport of growth species in the y direction only occurs as a result of gas phase diffusion (and thermodiffusion for the non-isothermal case). This follows directly from assumption 3.

Assumption 7. For all $x \geqslant 0$ the susceptor temperature is defined as T_s and the temperature at the top of the reactor is defined as T_0. Owing to the heating up of the cold gas the gas temperature at the beginning of the susceptor will be less than T_s. In practical situations one can correct this effect using pre-heating. In the present reactor set-up the susceptor temperature slowly increases until $x = 6$ cm and further remains constant. The entrance length of the temperature profile is of the same order, so that no extra errors are to be expected. The top of the reactor is water cooled so consequently the temperature will be practically constant (T_0).

Assumption 8. For all x no deposition occurs of growth species onto the top of the reactor. In the present reactor, however, deposition does occur. Analysis of the deposited layer shows that it mainly consists of As. Assuming that Ga growth species determine the growth rate (As is present in excess), this assumption seems correct.

Assumption 9. For all x and y the velocity profile $v(x, y, z, t)$, the temperature profile $T(x, y, z, t)$ and the concentration profile $C(x, y, z, t)$ are independent of z. This means that either a reactor is considered of infinite width or that no deposition occurs at the side walls of the reactor. This assumption reduces the problem to a two-dimensional one. Figure 3 illustrates the validity of this assumption. The flux of growth species at $y = 0$ is determined by the y-component of the diffusion in the y–z plane. This flux is in general a function of z. If no deposition on side walls occurs, reflection will take place. From symmetry considerations it follows that the flux of species towards the susceptor is independent of z. A more thorough derivation is given in appendix 1. In practice deposition on side walls does take place. In appendix 1 it is shown that this effect is small; hence the growth rate over the largest part of the width of the reactor is constant. A much stronger effect is seen in the corners of the reactor. For the present reactor (width 5 cm, height 2 cm, length 25 cm) this effect only extends a few mm inwards from the edges of the reactor. The effect of side walls on the temperature profile is much more difficult to determine. There will always be a heat loss through the side walls. Taking this effect into account in designing the heater of the reactor, the effect can be confined to a small region near the edges. Altogether the effect of the side walls is that over typically 90% of the total width of the reactor the growth rate will be constant.

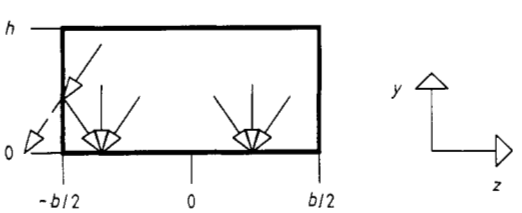

Figure 3. Flux of growth species in y–z plane. If no deposition on side walls occurs, reflection will take place.

Assumption 10. For all $x < 0$ no deposition occurs at the susceptor, while for $x \geqslant 0$ homogeneous deposition takes places on the susceptor and substrates. To obtain homogeneous deposition the whole susceptor should be covered with substrates. Because of high substrate costs this will not be possible (and is not done) in practical situations. As long as the surface does not play an important role in the crystal growth process no deviations are expected.

Assumption 11. Transport of growth components in the x direction (axially) only takes place because of convective (x direction) laminar (y–z plane) gas flow. Appendix 2 treats the effect of axial diffusion in the case of a simple isothermal model. It is concluded that under normal conditions only small effects are to be expected [8].

Assumption 12. For all possible gas-phase reactions it is assumed that they are either very fast or very slow. Fast reactions lead to a gas phase in equilibrium. Slow reactions do not yield products of significance. If such a reaction is necessary for the crystal growth process, it will be surface catalysed.

On the basis of the above assumptions it follows that the velocity and temperature profiles are only a function of y: $v(x, y, z, t) \equiv v(y)$ and $T(x, y, z, t) \equiv T(y)$. The concentration profile for one gas phase component is only a function of x and y: $C_i(x, y, z, t) \equiv C(x, y)$.

2.2. Differential equations

The concentration profile $C(x, y)$ is found from the continuity equation (mass conservation) or diffusion equation [10], which can be written in its general form as (using assumption 1)

$$\frac{\partial n C_{tot}}{\partial t} + \nabla \cdot [n C_{tot} v] = \nabla \cdot \{D C_{tot} [\vec{\nabla} n + \alpha_T n(1 - n) \vec{\nabla} \ln T]\} \qquad (1)$$

where C_{tot} is the total gas-phase concentration ($= P/R_gT$), $n \equiv n(x, y, z, t)$ the mole fraction of growth species ($C(x, y, z, t) = n(x, y, z, t)C_{tot}$), $C \equiv C(x, y, z, t)$ the concentration of growth species, $v \equiv v(x, y, z, t)$ the flow velocity, $D \equiv D(T(x, y, z, t))$ the binary diffusion coefficient of the group III component, α_T the thermal diffusion factor, $T \equiv (x, y, z, t)$ the growth temperature, P the total pressure and R_g is the gas constant.

Note that this expression is valid both in the mass-transport-limited as well as in the kinetically limited regime, as surface reaction kinetics are introduced as a boundary condition. Gas-phase reactions can be included by adding at the right-hand side terms that represent the generation and annihilation of species by chemical reactions; however, this is done elsewhere [21, 22]. With the assumptions described in §2.1 from which it also follows that the total pressure P is constant ($P = 1$ atm in our case) equation (1) reduces to (rewriting to $C(x, y)$ as variable, using $n(x, y, z, t) \ll 1$ (assumption 1)) the following partial differential equation

$$v(y)\frac{\partial C(x, y)}{\partial x} = \frac{\partial}{\partial y}\left[D(T(y))\left(\frac{\partial C(x, y)}{\partial y} + (\alpha_T + 1)\frac{C(x, y)}{T(y)}\frac{\partial T(y)}{\partial y}\right)\right] \quad (2)$$

with the appropriate boundary conditions:

$$C(0, y) = (T_0/T(y))C_0 \qquad 0 \leqslant y \leqslant h \quad (3)$$

$$J(x, 0) = kC(x, y)|_{y=0} \qquad x > 0 \quad (4)$$

$$J(x, h) = 0 \quad (5)$$

where the flux $J(x, y)$ is given by

$$J(x, y) = D(T(y))\left(\frac{\partial C(x, y)}{\partial y} + (\alpha_T + 1)\frac{C(x, y)}{T(y)}\frac{\partial T(y)}{\partial y}\right). \quad (6)$$

The $(\alpha_T + 1)$ terms in equations (2) and (6) originate from the fact that the total pressure P is constant, whereas the total gas-phase concentration C_{tot} is a function of temperature (and thus of height). In the above equations k denotes the rate constant for a reaction that is limited by surface kinetics (assumption 12) and C_0 the input concentration of the group III component. Boundary condition equation (3) represents the sudden change in the temperature profile at $x = 0$ (assumptions 3, 4, 5 and 10). Boundary condition equation (4) is based on assumptions 10 and 12, boundary condition equation (5) on assumption 8. Assumptions 1, 2 and 9 lead to the following definition of the growth rate $R(x)$:

$$R(x) = J(x, 0). \quad (7)$$

The temperature profile is found from the general expression for the heat balance

$$\rho c_p v(x, y)\frac{\partial T(x, y)}{\partial x} = \frac{\partial}{\partial y}\left[\kappa_0\left(\frac{T(x, y)}{T_0}\right)^{\beta}\frac{\partial T(x, y)}{\partial y}\right] \quad (8)$$

where ρ is the density of gas, c_p the specific heat of gas, κ the heat transfer coefficient with temperature dependence $\kappa = \kappa_0(T(x, y)/T_0)^{\beta}$ and T_0 the temperature at the top of the reactor ($= T(x, h)$).

From assumption 5 (fully developed temperature profile) it follows that the left-hand term of equation (8) is zero. Solving equation (8) for the case $\beta = 0$ (no temperature dependence of the heat transfer coefficient κ) yields a linear temperature gradient in the y direction:

$$T(y) = T_s - (T_s - T_0)\frac{y}{h} \quad (9)$$

where T_s denotes the temperature of the substrate. This temperature profile is not dependent on diffusion processes and velocity profile. The real profile does not differ much from this linear temperature gradient, as has been found experimentally [5, 19].

3. Diffusion-limited growth models

In this section models are derived for the regime where the growth is limited by diffusion of the group III component in the gas phase towards the substrate. Surface reactions will be treated in §4. Therefore the boundary condition equation (4) is simplified to $J(x, 0) = 0$. Furthermore the models are derived in the isothermal case with $T(y) \equiv T \equiv$ constant. The effect of a vertical temperature gradient is treated elsewhere [16]. It follows that thermal diffusion is automatically ignored as the temperature-dependent term in equations (2) and (6) equals zero ($(\partial/\partial y)\, T(y) = 0$). The velocity profile $v(y)$ in this case is parabolic. It will be shown that it is possible to solve equation (2) with the parabolic profile in the isothermal case. As this is rather complicated, we first derive simpler models that use increasingly better approximations of the parabolic profile. The six velocity profiles that are used (plug flow, linear flow, combinations of plug and linear flow, parabolic flow) are surveyed in figure 4. It will be shown in successive subsections that the growth rate can be expressed in general terms for all models. From this expression an important parameter can be deduced which is a measure of the amount of growth species that are actually incorporated and which is used as a check of the validity of the models. Therefore this parameter will be derived first. Next the various models are derived.

The equations concerning concentration $C(x, y)$ and growth rate $R(x)$ as functions of (x, y) and x, respectively, will be written using a number of dimensionless parameters, such as x/h, y/h, $D(T(y))/v_0h$, $C(x, y)/C_0$ and $R(x)/v_0C_0$, in order to obtain results that are more generally applicable.

3.1. General properties and total deposition check parameter ω

For all models it will be shown that the growth rate is expressed as a summation of terms, given by (note the dimensionless parameters)

$$R(x) = \sum_{i=1}^{\infty} A_i \exp(-B_i x). \quad (10)$$

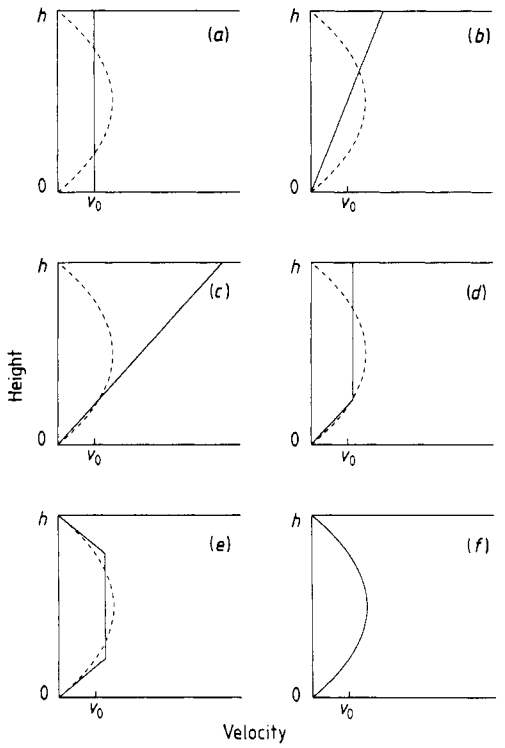

Figure 4. Survey of the six velocity profiles to be used in the models: (*a*) plug flow, constant velocity v_0, model 1; (*b*) linear profile I, $v(y) = 2v_0$, correct mass flux, model 2; (*c*) linear profile II, $v(y) = 4.5v_0$, approximation of parabolic profile in the region $0 \leqslant y/h \leqslant \frac{1}{4}$, model 3 [4]; (*d*) asymmetric combination of adapted linear profile II and plug flow with correct mass flux, model 4; (*e*) symmetric combination of adapted linear profile II and plug flow with correct mass flux, model 5; (*f*) parabolic profile $v(y) = 6v_0(y/h)(1 - (y/h))$, model 6. The broken curve in (*a*)–(*e*) represents the parabolic profile.

In most cases it suffices to use only one term, thus

$$R(x) = A \exp(-Bx). \tag{11}$$

Furthermore it will be shown that A is proportional to the input concentration of the group III component C_0 and that B is inversely proportional to $v_0 h$:

$$A = A'C_0 \qquad B = B'/v_0 h. \tag{12}$$

A model is believed to be valid and correct if it meets the condition that all growth species are built into the crystal if a reactor of infinite length is used. The 'total deposition check' parameter ω, defined as

$$\omega = \int_0^\infty R(x) b \, \mathrm{d}x / b h v_0 C_0 \tag{13}$$

is a measure of the validity of the model: the total amount of input growth species ($N_0 \equiv bhv_0C_0$) must equal the total amount of incorporated species. Therefore ω should be equal to 1. Substituting the previous expression for the growth rate equation (11) in equation (13) yields

$$\omega = A'/B'. \tag{14}$$

If the growth rate is expressed with more than one term (equation (10)) an expression for ω_n can be derived, where the suffix n denotes the number of terms used:

$$\omega_n = \sum_{i=1}^{n} A_i/B_i. \tag{15}$$

It should furthermore be noted that ω_∞ equals ω by definition. The total deposition check ω is a useful tool in determining the validity of a model and will be used throughout this series of papers.

3.2. Model 1, plug-flow profile

The case of a constant velocity profile $v(y) \equiv v_0$, see figure 4(*a*), also known as plug flow, results in a partial differential equation that is a considerable simplification of equation (2). This equation can be solved using the separation of variables method. Introducing the coordinate p ($p = y/h$) yields the following partial differential equation to be solved:

$$\frac{v_0 h^2}{D(T)} \frac{\partial C(x,p)}{\partial x} = \frac{\partial^2 C(x,p)}{\partial p^2} \tag{16}$$

with the appropriate boundary conditions:

$$C(0,p) = C_0 \tag{17}$$

$$C(x,0) = 0 \tag{18}$$

$$\left.\frac{\partial C(x,p)}{\partial p}\right|_{p=1} = 0. \tag{19}$$

Substitution of $C(x,p) = X(x)P(p)$ in the partial differential equation (16), rearranging and equating to (with a modest amount of foresight) $-\lambda^2$ yields:

$$\frac{v_0 h^2}{D(T)} \frac{1}{X(x)} \frac{\mathrm{d}X(x)}{\mathrm{d}x} = \frac{1}{P(p)} \frac{\mathrm{d}^2 P(p)}{\mathrm{d}p^2} = -\lambda^2. \tag{20}$$

The solution of equation (20) can be given as

$$X(x) = \exp\left(-\lambda^2 \frac{D(T)}{v_0 h} \frac{x}{h}\right) \tag{21}$$

$$P(p) = \alpha \sin(\lambda p) + \beta \cos(\lambda p). \tag{22}$$

From boundary condition equation (18) it follows that $\beta = 0$; boundary condition equation (19) leads to

$$\lambda_n = \frac{2n-1}{2}\pi \qquad \text{with } n = 1, 2, 3 \ldots.$$

The general solution of the partial differential equation (16) is found from a linear combination of all separate solutions:

$$C(x,p) = C_0 \sum_{n=1}^{\infty} \alpha_n \sin\left(\frac{2n-1}{2}\pi p\right) \times \exp\left(-\frac{(2n-1)^2\pi^2}{4} \frac{D(T)}{v_0 h} \frac{x}{h}\right). \tag{23}$$

From boundary condition equation (17) α_n can be calculated:

$$C_0 = C_0 \sum_{n=1}^{\infty} \alpha_n \sin\left(\frac{2n-1}{2}\pi p\right). \tag{24}$$

This is a Fourier series in p, transformation gives

$$\alpha_n = 2\int_0^1 \sin\left(\frac{2n-1}{2}\pi p\right) dp$$
$$= -2\frac{2}{(2n-1)\pi}\cos\left(\frac{2n-1}{2}\pi p\right)\Big|_0^1$$
$$= \frac{4}{\pi}\frac{1}{2n-1}. \qquad (25)$$

Substitution of equation (25) into equation (23) and back to (x, y) coordinates gives the complete solution of the partial differential equation (16) that had to be solved:

$$C(x, y) = \frac{4}{\pi} C_0 \sum_{n=1}^{\infty} \frac{1}{2n-1} \sin\left(\frac{2n-1}{2}\pi\frac{y}{h}\right)$$
$$\times \exp\left(-\frac{(2n-1)^2\pi^2}{4}\frac{D(T)}{v_0 h}\frac{x}{h}\right). \qquad (26)$$

The growth rate $R(x)$ is derived using its definition equation (7):

$$\frac{R(x)}{v_0 C_0} = 2\frac{D(T)}{v_0 h}\sum_{n=1}^{\infty}\exp\left(-\frac{(2n-1)^2\pi^2}{4}\frac{D(T)}{v_0 h}\frac{x}{h}\right). \qquad (27)$$

In figures 5 and 6 the dimensionless function $C(x, y)/C_0$ is shown as function of the three dimensionless parameters $(D(T)/v_0h)(x/h)$, n and y/h. Figure 5 shows $C(x, y)/C_0$ (dimensionless) as a function of y/h with $(D(T)/v_0h)(x/h)$ as parameter. The depletion of the concentration is shown in figure 6, where $C(x, y)/C_0$ is plotted as a function of $(D(T)/v_0h)(x/h)$ at different heights in the reactor (y/h). From figures 5 and 6 it follows that for $(D(T)/v_0h)(x/h) < 0.2$ larger values of n yield better results, i.e. a more realistic concentration profile, and that large values (> 10) of n should be used for $(D(T)/v_0h)(x/h) < 0.2$ in the calculation of the concentration profile and consequently the growth rate. For $(D(T)/v_0h)(x/h) > 0.2$ it suffices to use $n = 1$. If one examines $(R(x)/v_0C_0)(v_0h/D(T))$ (dimensionless) as a function of $(D(T)/v_0h)(x/h)$ with n as parameter (figure 7), it follows that in the region $(D(T)/v_0h)(x/h) < 0.2$ the effects of using large values of n is exhibited only in this region, which holds for the concentration profile as well. The region $(D(T)/v_0h)(x/h) < 0.2$ can thus be considered as the entrance region. In practical situations $(x/h \geq 4.0)$ using $n = 1$ will yield good results.

The growth rate $R(x)$ can be rewritten in a more general form as

$$\frac{R(x)}{v_0 C_0} = \frac{D(T)}{v_0 h}\sum_{n=1}^{\infty} A_n \exp\left(-B_n\frac{D(T)}{v_0 h}\frac{x}{h}\right) \qquad (28)$$

with, for model 1

$$A_n = 2$$
$$B_n = (2n-1)^2\pi^2/4.$$

The values of A_n and B_n are easily calculated and are

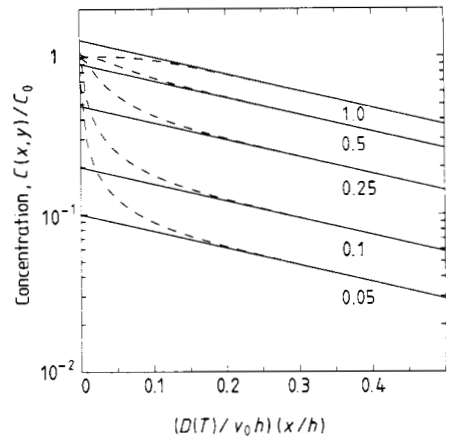

Figure 6. $C(x, y)/C_0$ as a function of $(D(T)/v_0h)(x/h)$ with y/h as parameter. The depletion of the concentration at different heights (y/h) is shown for $n = 1$ (full curves) and $n = 10$ (broken curves).

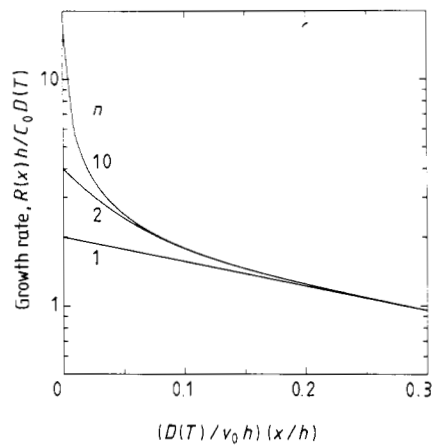

Figure 7. $R(x)h/C_0D(T)$ as a function of $(D(T)/v_0h)(x/h)$ with n as parameter. For $x/h > 0.2$ it suffices to use $n = 1$.

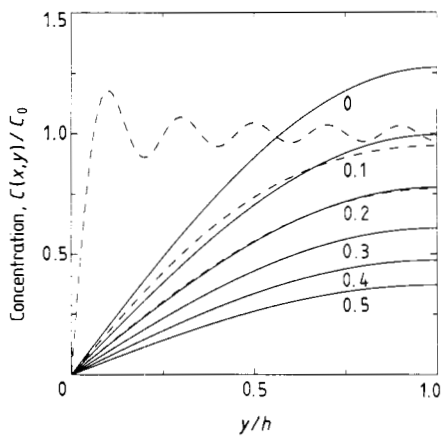

Figure 5. $C(x, y)/C_0$ as a function of y/h with $(D(T)/v_0h)(x/h)$ as parameter. The effect of different values of $(D(T)/v_0h)(x/h)$ is shown for $n = 1$ (full curves) and $n = 10$ (broken curves). For $(D(T)/v_0h)(x/h) > 0.2$ the differences between the $n = 1$ and the $n = 10$ curve can safely be neglected: the sinusoidal fluctuations, present at $(D(T)/v_0h)(x/h) = 0.0$, disappear completely at values beyond 0.2.

Table 1. Parameters of model 1.

n	A_n	B_n	ω_n
1	2	2.467	0.811
2	2	22.207	0.901
3	2	61.685	0.933
4	2	120.903	0.950
5	2	199.859	0.960

given in table 1. Taking into account all terms it can be calculated that [23]

$$\omega_\infty \equiv \omega = \frac{\int_0^\infty R(x)b\,\mathrm{d}x}{bhv_0C_0} = \frac{8}{\pi^2}\sum_{n=1}^{\infty}\frac{1}{(2n-1)^2} = 1. \quad (29)$$

When only the first term is used in the calculation of the growth rate, we obtain

$$\frac{R(x)}{v_0C_0} = 2\frac{D(T)}{v_0h}\exp\left(-2.467\frac{D(T)}{v_0h}\frac{x}{h}\right) \quad (30)$$

so that $\omega_1 = (A_1/B_1) = 0.811$.

3.3. Model 2, linear velocity profile (I)

The velocity profile $v(y)$ is a linear function of y such that the total mass flux through the reactor equals the mass flux in the case of the parabolic profile, or

$$\int_0^h v(y)\,\mathrm{d}y = v_0h. \quad (31)$$

The velocity at the substrate surface is zero, hence

$$v(y) = 2v_0y/h. \quad (32)$$

This velocity profile is depicted in figure 4(*b*). Coordinate transformation ($p = y/h$), substitution of $C(x, p) = X(x)P(p)$ in the partial differential equation (16) and use of the velocity profile equation (32) yields

$$\frac{2v_0h^2}{D(T)}\frac{1}{X(x)}\frac{\mathrm{d}X(x)}{\mathrm{d}x} = \frac{1}{P(p)p}\frac{\mathrm{d}^2P(p)}{\mathrm{d}p^2} = -\lambda^2. \quad (33)$$

The left-hand term can be solved to yield

$$X(x) = \exp\left(-\frac{\lambda^2}{2}\frac{D(T)}{v_0h}\frac{x}{h}\right). \quad (34)$$

The right-hand term can be solved using Bessel functions; first this term must be rewritten as

$$p^2\frac{\mathrm{d}^2P(p)}{\mathrm{d}p^2} + \lambda^2p^3P(p) = 0. \quad (35)$$

The solutions can be found in [24]:

$$P(p) = p^{1/2}[\alpha J_{1/3}(\tfrac{2}{3}\lambda p^{3/2}) + \beta J_{-1/3}(\tfrac{2}{3}\lambda p^{3/2})] \quad (36)$$

where $J_n(x)$ is a Bessel function of the first kind of order n. The constants α and β are to be determined still from boundary conditions equations (17)-(19). From boundary condition equation (18) it follows that $P(0) = 0$, hence $\beta = 0$. From boundary condition equation (19) and some algebra based on recurrence formulas of Bessel functions [24] it follows that

$$\left.\frac{\mathrm{d}P(p)}{\mathrm{d}p}\right|_{p=1} = \frac{\alpha}{(\frac{2}{3}\lambda)^{1/3}}\frac{\mathrm{d}[(\frac{2}{3}\lambda p^{3/2})^{1/3}J_{1/3}(\frac{2}{3}\lambda p^{3/2})]}{\mathrm{d}(\frac{2}{3}\lambda p^{3/2})} \times \left.\frac{\mathrm{d}(\frac{2}{3}\lambda p^{3/2})}{\mathrm{d}p}\right|_{p=1}$$
$$= pJ_{-2/3}(\tfrac{2}{3}\lambda p^{3/2})|_{p=1} = 0$$
$$\Rightarrow J_{-2/3}(\tfrac{2}{3}\lambda) = 0. \quad (37)$$

The roots λ_n of equation (37) can be found numerically. The five smallest values are given in table 2. The concentration $C(x, p)$ is now given by

$$C(x, p) = C_0\sum_{n=1}^{\infty}\alpha_np^{1/2}J_{1/3}(\tfrac{2}{3}\lambda_np^{3/2})\exp\left(-\tfrac{1}{2}\lambda_n^2\frac{D(T)}{v_0h}\frac{x}{h}\right). \quad (38)$$

The prefactor α_n can be found by substituting equation (38) in the boundary condition equation (17). This gives

$$C_0 = C_0\sum_{n=1}^{\infty}\alpha_np^{1/2}J_{1/3}(\tfrac{2}{3}\lambda_np^{3/2}). \quad (39)$$

Multiplication of both the left- and right-hand terms with $pJ_{1/3}(\frac{2}{3}\lambda_mp^{3/2})$ and integration with $p^{3/2}$ as integration variable yields

$$\int_0^1 pC_0J_{1/3}(\tfrac{2}{3}\lambda_mp^{3/2})\,\mathrm{d}p^{3/2} = \sum_{n=1}^{\infty}\alpha_n\int_0^1 p^{3/2}J_{1/3}(\tfrac{2}{3}\lambda_mp^{3/2})J_{1/3}(\tfrac{2}{3}\lambda_np^{3/2})\,\mathrm{d}p^{3/2}. \quad (40)$$

The right-hand term equals zero for $n \neq m$. For $n = m$ the right-hand term equals $\frac{1}{2}\alpha_nJ_{1/3}^2(\frac{2}{3}\lambda_n)$ (see [24]). Hence with $q = \frac{2}{3}\lambda_np^{3/2}$ it follows that

$$\alpha_n = \frac{2}{(\frac{2}{3}\lambda_n)^{5/3}}\frac{1}{J_{1/3}^2(\frac{2}{3}\lambda_n)}\int_0^{(2/3)\lambda_n}q^{2/3}J_{1/3}(q)\,\mathrm{d}q. \quad (41)$$

It can be derived that

$$\int_0^{(2/3)\lambda_n}q^{2/3}J_{1/3}(q)\,\mathrm{d}q = -q^{2/3}J_{-2/3}(q)|_0^{(2/3)\lambda_n}$$
$$= 0 + \lim_{q\to 0}q^{2/3}J_{-2/3}(q)$$
$$= \frac{2^{2/3}}{3\Gamma(\frac{4}{3})} \quad (42)$$

Table 2. Parameters of model 2.

n	λ_n	A_n	B_n	ω_n
1	1.8646	1.604	1.738	0.923
2	6.6437	1.012	22.069	0.969
3	11.3692	0.844	64.629	0.982
4	16.0871	0.751	129.397	0.988
5	20.7995	0.704	216.310	0.991

so that

$$\alpha_n = \frac{3^{2/3}}{\Gamma(\frac{4}{3})\lambda_n^{5/3} J_{1/3}^2(\frac{2}{3}\lambda_n)}. \tag{43}$$

The growth rate $R(x)$ can now be given as

$$\begin{aligned}\frac{R(x)}{v_0 C_0} &= \frac{D(T)}{v_0 h}\left.\frac{\partial C(x,p)}{\partial p}\right|_{p=0} \\ &= \frac{3^{2/3}}{\Gamma(\frac{4}{3})h}\frac{D(T)}{v_0 h}\sum_{n=1}^{\infty} \\ &\quad \times \left[\exp\left(-\tfrac{1}{2}\lambda_n^2 \frac{D(T)}{v_0 h}\frac{x}{h}\right)\Big/ \lambda_n^{5/3} J_{1/3}^2(\tfrac{2}{3}\lambda_n)\right] \\ &\quad \times \lim_{p\to 0}[pJ_{-2/3}(\tfrac{2}{3}\lambda_n p^{3/2})\lambda_n].\end{aligned} \tag{44}$$

Equation (44) can be written in its general form (equation (28)) to yield:

$$\frac{R(x)}{v_0 C_0} = \frac{D(T)}{v_0 h}\sum_{n=1}^{\infty} A_n \exp\left(-B_n \frac{D(T)}{v_0 h}\frac{x}{h}\right) \tag{45}$$

with

$$A_n = \frac{3^{1/3}}{\Gamma^2(\frac{4}{3})\lambda_n^{4/3} J_{1/3}^2(\frac{2}{3}\lambda_n)} \tag{46}$$

$$B_n = \tfrac{1}{2}\lambda_n^2. \tag{47}$$

Values for A_n and B_n are given in table 2 for $n = 1$ to 5. From these values it is clear that already for relatively small values of x the first term of equation (45) gives a sufficiently good description for the growth rate, hence

$$\frac{R(x)}{v_0 C_0} = 1.604\frac{D(T)}{v_0 h}\exp\left(-1.738\frac{D(T)}{v_0 h}\frac{x}{h}\right). \tag{48}$$

Performing the total deposition check of equation (48) yields $\omega_1 = 0.923$; values of ω_n for $n = 1$ to 5 are given in table 2.

3.4. Model 3, linear velocity profile (II)

In this model—previously used in our group by van de Ven *et al* [4]—the velocity profile $v(y)$ is also a linear function of y in such a way, however, that it gives a good approximation of the parabolic profile for small values of the height y (see figure 4(*c*)). For $0 \leqslant y \leqslant \frac{1}{4}h$ an error of $\simeq 10\%$ is made [4], if the following velocity profile is used:

$$v(y) = 4.5 v_0 y/h. \tag{49}$$

The derivation of the expression for the growth rate $R(x)$ is analogous to the one of model 2, hence (only the first term is given)

$$\frac{R(x)}{v_0 C_0} = 1.604\frac{D(T)}{v_0 h}\exp\left(-0.772\frac{D(T)}{v_0 h}\frac{x}{h}\right). \tag{50}$$

The total deposition check yields $\omega_1 = 2.08$, which is an unrealistic figure, resulting from the fact that this velocity profile approximates the parabolic profile only for small values of the height y ($0 \leqslant y \leqslant \frac{1}{4}h$) and not for all values. The total mass flux through the reactor is more than twice the mass flux in the case of the parabolic profile.

3.5. Model 4, asymmetric combination of linear velocity profile and plug flow

To approximate the parabolic profile just above the susceptor ($0 \leqslant y \leqslant \frac{1}{4}h$) and at the same time to obtain a correct total mass flux, a linear velocity profile is combined with a plug-flow profile to obtain the following asymmetric velocity profile (see figure 4(*d*)):

$$\begin{aligned} v(y) &= \tfrac{32}{7}v_0 y/h \qquad && 0 \leqslant y \leqslant \tfrac{1}{4}h \\ &= \tfrac{8}{7}v_0 && \tfrac{1}{4}h \leqslant y \leqslant h. \end{aligned} \tag{51}$$

The set of boundary conditions equations (17)–(19) is extended with two conditions that represent the continuity of the concentration profile $C(x, y)$ at $y = \frac{1}{4}h$, thus

$$\begin{aligned} C|_{y\uparrow h/4} &= C|_{y\downarrow h/4} \\ \left.\frac{\partial C}{\partial y}\right|_{y\uparrow h/4} &= \left.\frac{\partial C}{\partial y}\right|_{y\downarrow h/4}. \end{aligned} \tag{52}$$

Coordinate transformation ($p = y/h$), substitution of $C(x, p) = X(x)P(p)$ in the partial differential equation (16) and using the velocity profile equation (51) yields for the two regions:

(i) $0 \leqslant p \leqslant \frac{1}{4}$ (region 1).
Analogous to §3.3 it follows

$$\frac{\frac{8}{7}v_0 h^2}{D(T)}\frac{1}{X_1(x)}\frac{\mathrm{d}X_1(x)}{\mathrm{d}x} = \frac{1}{4P_1(p)p}\frac{\mathrm{d}^2 P_1(p)}{\mathrm{d}p^2} = -\lambda^2. \tag{53}$$

From boundary condition equation (18) ($p = 0$) the concentration profile in region 1 $C_1(x, y)$ is obtained:

$$C_1(x, p) = C_0\sum_{n=1}^{\infty}\alpha_n P_1(p)X_1(x) \tag{54}$$

with

$$\begin{aligned} P_1(p) &= p^{1/2}J_{1/3}(\tfrac{4}{3}\lambda_n p^{3/2}) \\ X_1(x) &= \exp\left(-\frac{7}{8}\lambda_n^2\frac{D(T)}{v_0 h}\frac{x}{h}\right). \end{aligned} \tag{55}$$

(ii) $\frac{1}{4} \leqslant p \leqslant 1$ (region 2).
Analogous to §3.2 it follows

$$\frac{\frac{8}{7}v_0 h^2}{D(T)}\frac{1}{X_2(x)}\frac{\mathrm{d}X_2(x)}{\mathrm{d}x} = \frac{1}{P_2(p)}\frac{\mathrm{d}^2 P_2(p)}{\mathrm{d}p^2} = -\mu^2 \tag{56}$$

with the solutions

$$\begin{aligned} P_2(p) &= \alpha' \cos(\mu p) + \beta' \sin(\mu p) \\ X_2(x) &= \exp\left(-\frac{7}{8}\mu^2\frac{D(T)}{v_0 h}\frac{x}{h}\right). \end{aligned} \tag{57}$$

From boundary condition equation (19) ($p = 1$) it follows

$$\begin{aligned} \alpha' &= \beta' \cot(\mu) \\ \Rightarrow P_2(p) &= \cos[\mu(1-p)]. \end{aligned} \tag{58}$$

The concentration profile in region 2, $C_2(x, y)$, is then given as

$$C_2(x, p) = C_0 \sum_{m=1}^{\infty} \alpha'_m P_2(p) X_2(x). \tag{59}$$

Using the extra boundary conditions equation (52) at $p = \frac{1}{4}$ yields

$$\sum_{n=1}^{\infty} \tfrac{1}{2}\alpha_n J_{1/3}(\tfrac{1}{6}\lambda_n) \exp\left(-\frac{7}{8}\lambda_n^2 \frac{D(T)}{v_0 h}\frac{x}{h}\right)$$
$$= \sum_{m=1}^{\infty} \alpha'_m \cos(\tfrac{3}{4}\mu_m) \exp\left(-\frac{7}{8}\mu_m^2 \frac{D(T)}{v_0 h}\frac{x}{h}\right)$$
$$\sum_{n=1}^{\infty} \tfrac{1}{2}\alpha_n J_{-2/3}(\tfrac{1}{6}\lambda_n) \exp\left(-\frac{7}{8}\lambda_n^2 \frac{D(T)}{v_0 h}\frac{x}{h}\right)$$
$$= \sum_{m=1}^{\infty} \alpha'_m \sin(\tfrac{3}{4}\mu_m) \exp\left(-\frac{7}{8}\mu_m^2 \frac{D(T)}{v_0 h}\frac{x}{h}\right). \tag{60}$$

The concentration profiles in both regions are coupled for all $x \geqslant 0$; from this it follows that all corresponding terms $(n = m)$ of $C_1(x, y)$ and $C_2(x, y)$ are coupled. Hence, for all $n = 1, 2, 3, \ldots$ it holds

$$\lambda_n = \mu_n \tag{61}$$

and therefore

$$\begin{aligned} \tfrac{1}{2}\alpha_n J_{1/3}(\tfrac{1}{6}\lambda_n) &= \alpha'_n \cos(\tfrac{3}{4}\lambda_n) \\ \tfrac{1}{2}\alpha_n J_{-2/3}(\tfrac{1}{6}\lambda_n) &= \alpha'_n \sin(\tfrac{3}{4}\lambda_n). \end{aligned} \tag{62}$$

The roots λ_n and the ratio α_n/α'_n can be found numerically. The five smallest values are given in table 3. The boundary condition equation (17) gives

$$\begin{aligned} C_0 = C_0 \sum_{n=1}^{\infty} \alpha_n p^{1/2} J_{1/3}(\tfrac{4}{3}\lambda_n p^{3/2}) \qquad & 0 \leqslant p \leqslant \tfrac{1}{4} \\ = C_0 \sum_{n=1}^{\infty} \alpha'_n \cos[\lambda_n(1-p)] \qquad & \tfrac{1}{4} \leqslant p \leqslant 1. \end{aligned} \tag{63}$$

From equation (63) in principle α_n and α'_n can be found. This is a complicated procedure, however. Therefore a least-squares fit (F) procedure is used to obtain reasonable estimates of α_n and α'_n. First a limited number of terms (k) is used in calculating equation (63). Then for a large number of values for p (e.g. 100) the relative difference $(C_{\text{calc}}(0, p_i) - C_0)$ is calculated. Subsequently the square of this difference is minimised with the k parameters α'_n (or α_n):

$$F_k^2 = \sum_i \left(\frac{C_{\text{calc}}(0, p_i) - C_0}{C_0}\right)^2 \text{ to be minimised.} \tag{64}$$

The result of this procedure for α'_n is shown in table 4, for $1 \leqslant k \leqslant 5$. From this it is clear that F_k^2 goes to zero very fast for increasing k; consequently the values for α'_n converge rapidly. The values for α_n can be found now using the already calculated (table 3) ratio α_n/α'_n. This is done in table 5. The growth rate $R(x)$ is now given as

$$\begin{aligned} \frac{R(x)}{v_0 C_0} &= \frac{D(T)}{v_0 h}\left.\frac{\partial C_1(x, p)}{\partial p}\right|_{p=0} \\ &= 2\frac{D(T)}{v_0 h}\sum_{n=1}^{\infty} \alpha_n \lambda_n \exp\left(-\frac{7}{8}\lambda_n^2 \frac{D(T)}{v_0 h}\frac{x}{h}\right) \\ &\quad \times \lim_{p\to 0}[pJ_{-2/3}(\tfrac{4}{3}\lambda_n p^{3/2})\lambda_n] \\ &= \frac{(2/3)^{1/3}}{\Gamma(\frac{4}{3})}\frac{D(T)}{v_0 h}\sum_{n=1}^{\infty} \alpha_n \lambda_n^{1/3} \exp\left(-\frac{7}{8}\lambda_n^2 \frac{D(T)}{v_0 h}\frac{x}{h}\right) \end{aligned} \tag{65}$$

or, in a general form

$$\frac{R(x)}{v_0 C_0} = \frac{D(T)}{v_0 h}\sum_{n=1}^{\infty} A_n \exp\left(-B_n \frac{D(T)}{v_0 h}\frac{x}{h}\right) \tag{66}$$

with

$$A_n = \frac{(2/3)^{1/3}}{\Gamma(\frac{4}{3})}\alpha_n \lambda_n^{1/3} \tag{67}$$

$$B_n = \tfrac{7}{8}\lambda_n^2. \tag{68}$$

The values of A_n and B_n are given in table 5 for $n = 1$ to 5. Already for relatively small values of x the first term of equation (65) gives a sufficiently good description for the growth rate, hence

$$\frac{R(x)}{v_0 C_0} = 1.899\frac{D(T)}{v_0 h}\exp\left(-2.172\frac{D(T)}{v_0 h}\frac{x}{h}\right). \tag{69}$$

Performing the total deposition check of equation (69) yields $\omega_1 = 0.874$; values of ω_n for $n = 1$ to 5 are given in table 5.

Table 3. Parameters of model 4.

n	λ_n	$\frac{7}{8}\lambda_n^2$	α_n/α'_n
1	1.5757	2.172	1.3501
2	4.8196	20.32	−2.4399
3	8.2126	59.02	2.9472
4	11.6818	119.4	−3.3754
5	15.1524	200.9	3.8864

Table 4. Least-squares fit of α'_n of model 4.

k	α'_1	α'_2	α'_3	α'_4	α'_5	F_k^2
1	1.2074					5.6373
2	1.2222	−0.2939				0.7706
3	1.2286	−0.3131	0.1139			0.1448
4	1.2332	−0.3238	0.1289	−0.0515		0.0326
5	1.2358	−0.3314	0.1386	−0.0624	0.0258	0.0080

Table 5. Parameters of model 4.

n	λ_n	α_n	α'_n	A_n	B_n	ω_n
1	1.5757	1.668	1.2358	1.899	2.172	0.874
2	4.8196	0.809	−0.3314	1.336	20.32	0.940
3	8.2126	0.408	0.1386	0.806	59.02	0.952
4	11.6818	0.211	−0.0624	0.468	119.4	0.956
5	15.1524	0.100	0.0258	0.243	200.9	0.957

3.6. Model 5, symmetric combination of linear velocity profile and plug flow

The linear velocity profile can be combined with plug flow in such a way that one obtains a symmetric profile. This is done to approximate the parabolic profile as well as possible. The velocity profile is divided into three regions, as follows (see figure 4(*e*)):

$$\begin{aligned} v(y) &= a_v v_0 y/h && 0 \leqslant y \leqslant \delta \\ &= b_v v_0 && \delta \leqslant y \leqslant h-\delta \\ &= a_v v_0\left(1-\frac{y}{h}\right) && h-\delta \leqslant y \leqslant h. \end{aligned} \tag{70}$$

The parameters a_v and b_v are found to be (the total mass flux equals $v_0 h$):

$$\begin{aligned} a_v &= \left[\frac{\delta}{h}\left(1-\frac{\delta}{h}\right)\right]^{-1} \\ b_v &= a_v \delta/h. \end{aligned} \tag{71}$$

In the special case that a_v is approximated by the slope of the tangent of the parabolic profile at $y = 0$ (i.e. $a_v = 6$) it follows that $\delta_{\text{parabolic}} = 0.211h$ and $b_v = 1.268$.

The set of boundary conditions equations (17)–(19) is extended with four conditions that represent the continuity of the concentration profile $C(x, y)$ at $y = \delta$ and $y = h - \delta$ thus

$$\begin{aligned} C|_{y\uparrow\delta} &= C|_{y\downarrow\delta} \\ \left.\frac{\partial C}{\partial y}\right|_{y\uparrow\delta} &= \left.\frac{\partial C}{\partial y}\right|_{y\downarrow\delta} \\ C|_{y\uparrow h-\delta} &= C|_{y\downarrow h-\delta} \\ \left.\frac{\partial C}{\partial y}\right|_{y\uparrow h-\delta} &= \left.\frac{\partial C}{\partial y}\right|_{y\downarrow h-\delta}. \end{aligned} \tag{72}$$

Coordinate transformation ($p = y/h$), substitution of $C(x, p) = X(x)P(p)$ in the partial differential equation (16) and using the velocity profile equation (70) yields for the three following regions.

(i) $0 \leqslant p \leqslant \delta/h$ (region 1).

Analogous to §3.3 it follows

$$\frac{a_v v_0 h^2}{D(T)} \frac{1}{X_1(x)} \frac{\mathrm{d}X_1(x)}{\mathrm{d}x} = \frac{1}{P_1(p)p} \frac{\mathrm{d}^2 P_1(p)}{\mathrm{d}p^2} = -\lambda^2. \tag{73}$$

From boundary condition equation (18) ($p = 0$) the concentration profile in region 1, $C_1(x, y)$, is obtained:

$$C_1(x, p) = C_0 \sum_{n=1}^{\infty} \alpha_n P_1(p) X_1(x) \tag{74}$$

with

$$\begin{aligned} P_1(p) &= p^{1/2} J_{1/3}(\tfrac{2}{3}\lambda_n p^{3/2}) \\ X_1(x) &= \exp\left(-\frac{1}{a_v}\lambda_n^2 \frac{D(T)}{v_0 h}\frac{x}{h}\right). \end{aligned} \tag{75}$$

(ii) $\delta/h \leqslant p \leqslant 1 - \delta/h$ (region 2).

Analogous to §3.2 it follows

$$\frac{b_v v_0 h^2}{D(T)} \frac{1}{X_2(x)} \frac{\mathrm{d}X_2(x)}{\mathrm{d}x} = \frac{1}{P_2(p)} \frac{\mathrm{d}^2 P_2(p)}{\mathrm{d}p^2} = -\mu^2. \tag{76}$$

The concentration profile in region 2, $C_2(x, y)$, is given as

$$C_2(x, p) = C_0 \sum_{m=1}^{\infty} \alpha'_m P_2(p) X_2(x) \tag{77}$$

with

$$\begin{aligned} P_2(p) &= \sin(\mu_m p) + (\beta'_m/\alpha'_m)\cos(\mu_m p) \\ X_2(x) &= \exp\left(-\frac{1}{b_v}\mu_m^2 \frac{D(T)}{v_0 h}\frac{x}{h}\right). \end{aligned} \tag{78}$$

(iii) $1 - \delta/h \leqslant p \leqslant 1$ (region 3).

It is more convenient to use the coordinate $p'(= 1 - p)$ instead of p in this region. It follows

$$\frac{a_v v_0 h^2}{D(T)} \frac{1}{X_3(x)} \frac{\mathrm{d}X_3(x)}{\mathrm{d}x} = \frac{1}{P_3(p')p'} \frac{\mathrm{d}^2 P_3(p')}{\mathrm{d}p'^2} = -\nu^2 \tag{79}$$

so that the concentration profile in region 3, $C_3(x, y)$, is given as

$$C_3(x, p') = C_0 \sum_{k=1}^{\infty} \alpha''_k P_3(p') X_3(x) \tag{80}$$

with

$$\begin{aligned} P_3(p') &= p'^{1/2}\left(\frac{\beta''_k}{\alpha''_k} J_{1/3}(\tfrac{2}{3}\nu_k p'^{3/2}) + J_{-1/3}(\tfrac{2}{3}\nu_k p'^{3/2})\right) \\ X_3(x) &= \exp\left(-\frac{1}{a_v}\nu_k^2 \frac{D(T)}{v_0 h}\frac{x}{h}\right). \end{aligned} \tag{81}$$

From boundary condition equation (19) ($p' = 0$) it follows that $\beta''_k = 0$, therefore:

$$P_3(p) = (1-p)^{1/2}[J_{-1/3}(\tfrac{2}{3}\nu_k(1-p)^{3/2})]. \tag{82}$$

The extra boundary conditions equation (72) at $p = \delta/h$ and $p' = \delta/h$ couple the concentration profiles in the three regions for all $x \geqslant 0$; therefore all corresponding terms ($n = m = k$) of $C_1(x, y)$, $C_2(x, y)$ and $C_3(x, y)$ are coupled. Hence, for all $n = 1, 2, 3, \ldots$, it follows

$$\lambda_n^2 = \nu_n^2 = \frac{a_v}{b_v}\mu_n^2 = \frac{h}{\delta}\mu_n^2. \tag{83}$$

Furthermore one obtains for every n:

$$\alpha_n\left(\frac{\delta}{h}\right)^{1/2} J_{1/3}\left(\frac{2}{3}\frac{\delta}{h}\mu_n\right) = \alpha'_n \sin\left[\left(\frac{\delta}{h}\right)\mu_n\right] + \beta'_n \cos\left[\left(\frac{\delta}{h}\right)\mu_n\right]$$

$$\alpha_n\left(\frac{\delta}{h}\right)^{1/2} J_{-2/3}\left(\frac{2}{3}\frac{\delta}{h}\mu_n\right) = \alpha'_n \cos\left[\left(\frac{\delta}{h}\right)\mu_n\right] - \beta'_n \sin\left[\left(\frac{\delta}{h}\right)\mu_n\right]$$

$$\alpha''_n\left(\frac{\delta}{h}\right)^{1/2} J_{-1/3}\left(\frac{2}{3}\frac{\delta}{h}\mu_n\right) = \alpha'_n \sin\left[\left(1-\frac{\delta}{h}\right)\mu_n\right] + \beta'_n \cos\left[\left(1-\frac{\delta}{h}\right)\mu_n\right]$$

$$\alpha_n''\left(\frac{\delta}{h}\right)^{1/2} J_{2/3}\left(\frac{2}{3}\frac{\delta}{h}\mu_n\right) = \alpha_n' \cos\left[\left(1-\frac{\delta}{h}\right)\mu_n\right] - \beta_n' \sin\left[\left(1-\frac{\delta}{h}\right)\mu_n\right]. \tag{84}$$

Some algebra then yields

$$\frac{\alpha_n'}{\beta_n'} = \frac{J_{1/3}\left(\frac{2}{3}\frac{\delta}{h}\mu_n\right)\sin\left[\left(\frac{\delta}{h}\right)\mu_n\right] + J_{-2/3}\left(\frac{2}{3}\frac{\delta}{h}\mu_n\right)\cos\left[\left(\frac{\delta}{h}\right)\mu_n\right]}{J_{1/3}\left(\frac{2}{3}\frac{\delta}{h}\mu_n\right)\cos\left[\left(\frac{\delta}{h}\right)\mu_n\right] - J_{-2/3}\left(\frac{2}{3}\frac{\delta}{h}\mu_n\right)\sin\left[\left(\frac{\delta}{h}\right)\mu_n\right]} \tag{85}$$

$$\tan\left[\mu_n\left(1-2\frac{\delta}{h}\right)\right] = \frac{J_{-1/3}\left(\frac{2}{3}\frac{\delta}{h}\mu_n\right)J_{-2/3}\left(\frac{2}{3}\frac{\delta}{h}\mu_n\right) - J_{1/3}\left(\frac{2}{3}\frac{\delta}{h}\mu_n\right)J_{2/3}\left(\frac{2}{3}\frac{\delta}{h}\mu_n\right)}{J_{1/3}\left(\frac{2}{3}\frac{\delta}{h}\mu_n\right)J_{-1/3}\left(\frac{2}{3}\frac{\delta}{h}\mu_n\right) + J_{2/3}\left(\frac{2}{3}\frac{\delta}{h}\mu_n\right)J_{-2/3}\left(\frac{2}{3}\frac{\delta}{h}\mu_n\right)}. \tag{86}$$

For every $\delta(0 \leqslant \delta \leqslant \frac{1}{2}h)$ the roots μ_n can be found using equation (86); the other parameters are determined using the boundary condition at the beginning of the reactor (equation (17)). In table 6 the parameters μ_n, α_n, α_n', β_n', α_n'', are calculated using $\delta = \delta_{\text{parabolic}} = 0.211h$. The growth rate $R(x)$ can now be given as

$$\begin{aligned}\frac{R(x)}{v_0 C_0} &= \frac{D(T)}{v_0 h}\left.\frac{\partial C_1(x,p)}{\partial p}\right|_{p=0} \\ &= \frac{D(T)}{v_0 h}\left(\frac{h}{\delta}\right)^{1/2}\sum_{n=1}^{\infty}\alpha_n\mu_n \exp\left(-\frac{1}{a_v}\mu_n^2\frac{h}{\delta}\frac{D(T)}{v_0 h}\frac{x}{h}\right) \\ &\quad\times \lim_{p\to 0} pJ_{-2/3}\left[\frac{2}{3}\mu_n\left(\frac{h}{\delta}\right)^{1/2}p^{3/2}\right] \\ &= \frac{(1/3)^{1/3}}{\Gamma(\frac{4}{3})}\frac{D(T)}{v_0 h}\sum_{n=1}^{\infty}\alpha_n\mu_n^{1/3}\left(\frac{h}{\delta}\right)^{1/6} \\ &\quad\times \exp\left(-\frac{1}{a_v}\mu_n^2\frac{h}{\delta}\frac{D(T)}{v_0 h}\frac{x}{h}\right)\end{aligned} \tag{87}$$

or, in a general form

$$\frac{R(x)}{v_0 C_0} = \frac{D(T)}{v_0 h}\sum_{n=1}^{\infty} A_n \exp\left(-B_n\frac{D(T)}{v_0 h}\frac{x}{h}\right) \tag{88}$$

with

$$A_n = \frac{(1/3)^{1/3}}{\Gamma(\frac{4}{3})}\left(\frac{h}{\delta}\right)^{1/6}\alpha_n\mu_n^{1/3} \tag{89}$$

$$B_n = \frac{1}{a_v}\mu_n^2\frac{h}{\delta} = \mu_n^2\left(1-\frac{\delta}{h}\right). \tag{90}$$

The values of A_n and B_n are given in table 6 for $n = 1$ to 5 using $\delta = \delta_{\text{parabolic}} = 0.211h$. Already for relatively small values of x the first term of equation (87) gives a sufficiently good description of the growth rate, hence

$$\frac{R(x)}{v_0 C_0} = 2.157\frac{D(T)}{v_0 h}\exp\left(-2.444\frac{D(T)}{v_0 h}\frac{x}{h}\right). \tag{91}$$

Performing the total deposition check of equation (91) using $\delta = \delta_{\text{parabolic}} = 0.211h$ yields $\omega_1 = 0.882$; values of ω_n for $n = 1$ to 5 are given in table 6.

The dependence of the parameters A_1 and B_1 on the value of δ/h is depicted in figure 8. For $\delta \to 0$ the parameters A_1 and B_1 approach the values calculated in the case of plug flow, which is to be expected. Note that the change in the exponential parameter B_1 is only 1% with respect to the B_1 as calculated for $\delta = \delta_{\text{parabolic}} = 0.211h$.

3.7. Model 6, parabolic velocity profile

The exact velocity profile in the diffusion-controlled regime in the isothermal case is parabolic [10] (see figure 4(*f*)):

$$v(y) = 6v_0\left[\frac{y}{h} - \left(\frac{y}{h}\right)^2\right] \tag{92}$$

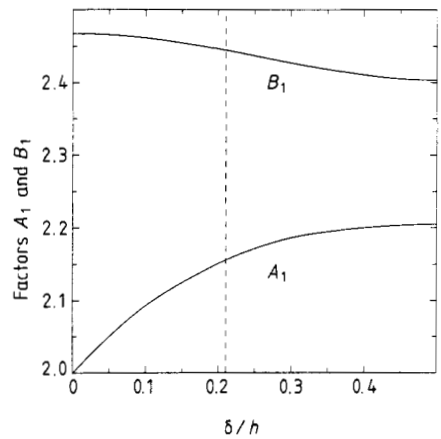

Figure 8. Parameters A_1 and B_1 of model 5 as a function of δ/h. The broken line indicates where $\delta = \delta_{\text{parabolic}} = 0.211h$.

Table 6. Parameters of model 5 ($\delta = \delta_{\text{parabolic}} = 0.211h$).

n	μ_n	α_n	α_n'	$10^3\beta_n'$	α_n''	A_n	B_n	ω_n
1	1.7605	1.776	1.252	5.271	1.849	2.157	2.444	0.882
2	5.3582	0.960	0.369	34.46	−0.832	1.689	22.65	0.957
3	9.0650	0.610	0.185	60.26	0.567	1.278	64.84	0.977
4	12.7941	0.443	−0.102	71.22	−0.451	1.041	129.2	0.985
5	16.4808	0.397	0.061	77.79	0.420	1.015	214.3	0.989

and the following partial differential equation is to be solved:

$$\frac{6v_0}{D(T)}\left[\frac{y}{h}-\left(\frac{y}{h}\right)^2\right]\frac{\partial C(x,p)}{\partial x}=\frac{\partial^2 C(x,y)}{\partial y^2}. \quad (93)$$

Coordinate transformation ($p = y/h$) and substitution of $C(x, p) = X(x)P(p)$ in the partial differential equation (93) yields

$$\frac{6v_0h^2}{D(T)}\frac{1}{X(x)}\frac{dX(x)}{dx}=\frac{1}{P(p)p(1-p)}\frac{d^2P(p)}{dp^2}=-\lambda^2. \quad (94)$$

The left-hand term of equation (94) results in

$$X(x)=\exp\left(-\frac{1}{6}\lambda^2\frac{D(T)}{v_0h}\frac{x}{h}\right). \quad (95)$$

The right-hand term can be solved using parabolic cylinder functions [25]; first this term must be rewritten as

$$\frac{d^2P(p)}{dp^2}+(-\lambda^2p^2+\lambda^2p)P(p)=0. \quad (96)$$

Equation (96) can be solved after a coordinate transformation $q=\sqrt{2\lambda}(p-\frac{1}{2})$ which gives

$$\frac{d^2P(p)}{dq^2}-\left(\frac{1}{4}q^2-\frac{\lambda}{8}\right)P(q)=0. \quad (97)$$

The solutions of equation (97) can be found in [25]:

$$P(q)=\alpha Y_1(q)+\beta Y_2(q) \quad (98)$$

with

$$\begin{aligned}Y_1(q)&=\exp\left(-\frac{1}{4}q^2\right)M\left(\frac{1}{4}-\frac{\lambda}{16};\frac{1}{2};\frac{1}{2}q^2\right)\\ Y_2(q)&=q\exp\left(-\frac{1}{4}q^2\right)M\left(\frac{3}{4}-\frac{\lambda}{16};\frac{3}{2};\frac{1}{2}q^2\right).\end{aligned} \quad (99)$$

Here $M(a; b; z)$ are the confluent hypergeometric functions [25], which can be generated with Kummer's function [25]:

$$M(a;b;z)=\sum_{n=0}^{\infty}\frac{(a)_n}{(b)_n}\frac{z^n}{n!} \quad (100)$$

where $(a)_n$ and $(b)_n$ are defined as

$$\begin{aligned}(a)_0&=1 \qquad (a)_n=(a)_{n-1}(a+n-1)\\ (b)_0&=1 \qquad (b)_n=(b)_{n-1}(b+n-1).\end{aligned} \quad (101)$$

Boundary condition equation (18) becomes after the coordinate transformation

$$P(q)|_{q=-(1/2)\sqrt{2\lambda}}=0$$

which leads to

$$\alpha=\frac{1}{2}\sqrt{2\lambda}\frac{M\left(\frac{3}{4}-\frac{\lambda}{16};\frac{3}{2};\frac{\lambda}{4}\right)}{M\left(\frac{1}{4}-\frac{\lambda}{16};\frac{1}{2};\frac{\lambda}{4}\right)}\beta. \quad (102)$$

Boundary condition equation (19) becomes

$$\left.\frac{dP(q)}{dq}\right|_{q=(1/2)\sqrt{2\lambda}}=0$$

leading to

$$\begin{aligned}\frac{2\lambda-4}{\lambda}&=\left(1-\frac{\lambda}{4}\right)\frac{M\left(\frac{5}{4}-\frac{\lambda}{16};\frac{3}{2};\frac{\lambda}{4}\right)}{M\left(\frac{1}{4}-\frac{\lambda}{16};\frac{1}{2};\frac{\lambda}{4}\right)}\\ &+\left(1-\frac{\lambda}{12}\right)\frac{M\left(\frac{7}{4}-\frac{\lambda}{16};\frac{5}{2};\frac{\lambda}{4}\right)}{M\left(\frac{3}{4}-\frac{\lambda}{16};\frac{5}{2};\frac{\lambda}{4}\right)}.\end{aligned} \quad (103)$$

From equations (102) and (103) the roots λ and the ratio β/α can be found numerically. Results are given in table 7. The concentration profile is now given by

$$\begin{aligned}C(x,q)=C_0\sum_{n=1}^{\infty}\alpha_n&\left(Y_1(q)+\frac{\beta_n}{\alpha_n}Y_2(q)\right)\\ &\times\exp\left(-\frac{1}{6}\lambda^2\frac{D(T)}{v_0h}\frac{x}{h}\right).\end{aligned} \quad (104)$$

With boundary condition equation (17) at the beginning of the reactor ($x = 0$) α_n can be found, using the least-squares fit as described in §3.5. Results are given in table 8. From this it is clear that F_k^2 goes to zero for increasing k; consequently the values for α_n converge. The values for β_n can be found now using the already calculated (table 7) ratio β_n/α_n. This is done in table 9. The growth rate

Table 7. Parameters of model 6.

n	λ_n	$\frac{1}{6}\lambda_n^2$	β_n/α_n
1	3.8187	2.430	0.5161
2	11.897	23.59	−2.0381
3	19.924	66.16	0.9580
4	27.938	130.1	−3.1499
5	35.947	215.4	1.2610

Table 8. Least-squares fit of α_n of model 6.

k	α_1	α_2	α_3	α_4	α_5	F_k^2
1	0.9497					16.6373
2	1.0253	0.1811				9.4987
3	0.9747	0.1953	−0.1808			6.8048
4	0.9867	0.1702	−0.1920	−0.0789		5.3842
5	0.9769	0.1743	−0.1595	−0.0829	0.1054	4.4926
9	0.9762	0.1681	−0.1525	−0.0647	0.0816	2.7836

Table 9. Parameters of model 6.

n	λ_n	α_n	β_n	A_n	B_n	ω_n
1	3.8187	0.9762	0.504	2.177	2.430	0.896
2	11.897	0.1681	−0.343	1.446	23.59	0.957
3	19.924	−0.1525	−0.146	1.218	66.16	0.976
4	27.938	−0.0647	0.204	1.143	130.1	0.984
5	35.947	0.0816	0.103	1.057	215.4	0.989

$R(x)$ can now be given as

$$\frac{R(x)}{v_0 C_0} = \frac{D(T)}{v_0 h}\left.\frac{\partial C(x,p)}{\partial p}\right|_{p=0}$$
$$= \frac{D(T)}{v_0 h}\sum_{n=1}^{\infty}\alpha_n\left[2M_1 - \frac{\lambda_n}{2}\left(1-\frac{\lambda_n}{4}\right)M_3 + \frac{\lambda_n}{2}\left(1-\frac{\lambda_n}{12}\right)\frac{M_1}{M_2}M_4\right] \times \exp\left(\frac{\lambda_n}{8}\right)\exp\left(-\frac{1}{6}\lambda_n^2\frac{D(T)}{v_0 h}\frac{x}{h}\right) \quad (105)$$

with

$$M_1 = M\left(\frac{1}{4}-\frac{\lambda_n}{16};\frac{1}{2};\frac{\lambda_n}{4}\right)$$
$$M_2 = M\left(\frac{3}{4}-\frac{\lambda_n}{16};\frac{3}{2};\frac{\lambda_n}{4}\right)$$
$$M_3 = M\left(\frac{5}{4}-\frac{\lambda_n}{16};\frac{3}{2};\frac{\lambda_n}{4}\right) \quad (106)$$
$$M_4 = M\left(\frac{7}{4}-\frac{\lambda_n}{16};\frac{5}{2};\frac{\lambda_n}{4}\right).$$

The general form then is

$$\frac{R(x)}{v_0 C_0} = \frac{D(T)}{v_0 h}\sum_{n=1}^{\infty}A_n\exp\left(-B_n\frac{D(T)}{v_0 h}\frac{x}{h}\right) \quad (107)$$

with

$$A_n = \alpha_n\left[2M_1 - \frac{\lambda_n}{2}\left(1-\frac{\lambda_n}{4}\right)M_3 + \frac{\lambda_n}{2}\left(1-\frac{\lambda_n}{12}\right)\frac{M_1}{M_2}M_4\right]\exp\left(\frac{\lambda_n}{8}\right) \quad (108)$$

$$B_n = \frac{1}{6}\lambda_n^2. \quad (109)$$

The values of A_n and B_n are given in table 9 for $n = 1$ to 5. For relatively small values of x the first term of equation (106) gives a sufficiently good description for the growth rate, hence

$$\frac{R(x)}{v_0 C_0} = 2.177\frac{D(T)}{v_0 h}\exp\left(-2.430\frac{D(T)}{v_0 h}\frac{x}{h}\right). \quad (110)$$

Performing the total deposition check of equation (111) yields $\omega_1 = 0.896$; values of ω_n for $n = 1$ to 5 are given in table 9.

3.8. Comparison between models 1, 2, 4, 5 and 6

From the previous subsections it follows that the growth rate $R(x)$ can always be written in the general form

$$\frac{R(x)}{v_0 C_0} = \frac{D(T)}{v_0 h}\sum_{n=1}^{\infty}A_n\exp\left(-B_n\frac{D(T)}{v_0 h}\frac{x}{h}\right) \quad (111)$$

where the constants A_n and B_n are determined by the velocity profile used. In nearly all cases the first term contributes more than 90% to the complete expression. Therefore it can be stated that in good approximation the growth rate can be described by

$$\frac{R(x)}{v_0 C_0} = A\frac{D(T)}{v_0 h}\exp\left(-B\frac{D(T)}{v_0 h}\frac{x}{h}\right) \quad (112)$$

as was already assumed in §3.1. Deviations appear to be small ($\sim 10\%$) and are caused mainly by the entrance region. In figure 9 the concentration profiles of models 1, 2, 4, 5 ($\delta = \delta_{\text{parabolic}}$) and 6 are plotted as a function of y/h at $(D(T)/v_0 h)(x/h) = 0.5$. For all models only the first term is used in the calculation. Taking into account models 1, 5 and 6, it is clear that the concentration curves differ only a few per cent. This stems from the fact that the velocity profile of these models is symmetric around $y/h = 0.5$. The same effect can be seen in figure 10, where the growth rate is shown as function of $(D(T)/v_0 h)(x/h)$ for models 1, 2, 4, 5 and 6. Here also the first term is used in the calculation only. The important conclusion that follows from these figures is that the parabolic velocity

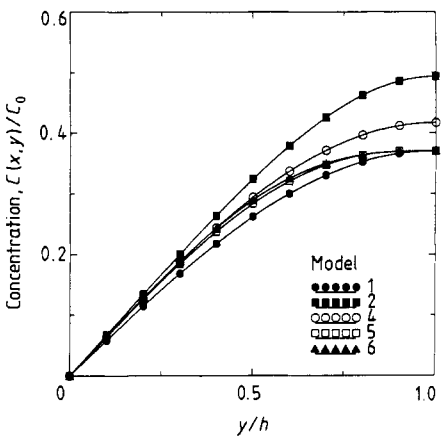

Figure 9. $C(x, y)/C_0$ as a function of y/h for the models 1, 2, 4, 5 ($\delta = \delta_{\text{parabolic}}$) and 6 at $(D(T)/v_0 h)(x/h) = 0.5$. The calculation is done using only the first term. Note that the results for models 1, 5 and 6 are roughly the same.

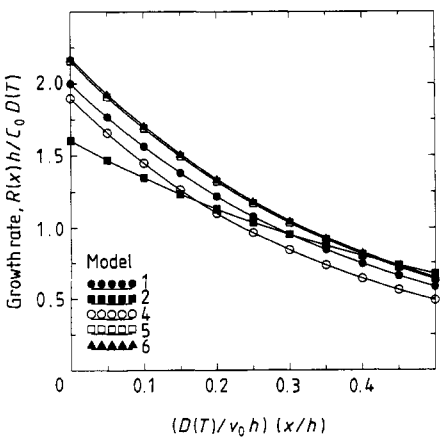

Figure 10. $R(x)h/C_0 D(T)$ as a function of $(D(T)/v_0 h)(x/h)$ for the models 1, 2, 4, 5 ($\delta = \delta_{\text{parabolic}}$) and 6. The calculation is done using only the first term. Note the close correspondence between models 5 ($\delta = \delta_{\text{parabolic}}$) and 6.

profile is best approximated using model 5 with $\delta = \delta_{parabolic} = 0.211h$. Furthermore it is clear that in the case of models 1, 5 and 6 the results are approximately the same (within $\sim 10\%$). This is an important observation, because it suggests that the plug-flow profile may be used instead of the parabolic profile to derive concentration profiles and growth rates. This facilitates the calculations considerably. The fact that the growth rate as calculated with models 1 (plug flow) and 5 agrees so well with the one as calculated with model 6 (parabolic flow) originates from the small differences of the first exponential terms B_1. This is due to the fact that these models possess a symmetric velocity profile. For convenience these terms (B) are listed again in table 10, where also the constant A is given for the models 1, 2, 4, 5 and 6. In conclusion it can be stated that although small errors are introduced in the calculations using the plug-flow profile, we still favour the use of this profile because of its simple, though realistic results. Therefore in following publications [16–18] the plug-flow profile will be used instead of the parabolic profile to derive concentration profiles and growth rates.

4. Influence of surface kinetics

In this section a model is derived for the regime where the growth is limited by a surface reaction. This model is then combined with the above described model for the diffusion-controlled regime (i.e. model 1, plug flow). Both models are derived in the isothermal case with $T(y) \equiv T \equiv$ constant.

4.1. Model 7, growth limited by surface kinetics

If the gas-phase diffusion is very fast in comparison with the surface reaction a homogeneous gas phase results: the concentration $C(x, y)$ has become independent of y (thus $C(x, y) \equiv C(x)$). If a first-order surface reaction or adsorption is assumed, with reaction rate constant k, the following differential equation results in

$$v_0 \frac{dC(x)}{dx} = -\frac{k}{h} C(x). \tag{113}$$

The rate constant k is a function of the substrate temperature T_s as follows:

$$k = \frac{k_B T_s}{h_P} \exp\left(-\frac{E_a}{R_g T_s}\right) \tag{114}$$

Table 10. Comparison of parameters A, B and ω_1 of models 1, 2, 4, 5 ($\delta = \delta_{parabolic}$) and 6.

Model	A	B	ω_1
1	2.000	2.467	0.811
2	1.604	1.738	0.923
4	1.899	2.172	0.874
5	2.157	2.444	0.882
6	2.177	2.430	0.896

where k_B is the Boltzmann constant, h_P the Planck constant and E_a the activation energy for the rate limiting step. Solving equation (113) using boundary condition equation (3) yields

$$C(x) = C_0 \exp\left(-\frac{k}{v_0}\frac{x}{h}\right). \tag{115}$$

The growth rate $R(x)$ then is given as (note that $R(x)/v_0 C_0$ is dimensionless)

$$\frac{R(x)}{v_0 C_0} = \frac{k}{v_0}\frac{C(x)}{C_0} = \frac{k}{v_0} \exp\left(-\frac{k}{v_0}\frac{x}{h}\right). \tag{116}$$

It will be clear that this model is (nearly) independent of the velocity and temperature profile of the gas phase. This model can be applied for the description of processes that are completely surface catalysed, e.g. MOVPE of GaAs at $T_s < 500$ °C.

4.2. Combination of growth limited by surface kinetics and diffusion-controlled growth, model 8

The two extreme cases, i.e. growth limited by surface kinetics (model 7) on the one hand and diffusion-controlled growth (model 1, plug flow) on the other, can easily be combined. The partial differential equation that is to be solved is the same as in previous sections (i.e. equation (16)). Note that the plug-flow profile is used. The only difference is that the boundary condition equation (18) (the concentration of growth species equals zero at the substrate surface) must be changed. Assuming a first-order reaction with reaction rate constant k the boundary condition now becomes (using $p = y/h$):

$$\frac{D(T_s)}{h}\frac{\partial C(x, p)}{\partial p}\bigg|_{p=0} = k(T_s)C(x, 0). \tag{117}$$

This can be rewritten using the well-known dimensionless CVD number [26, 27]

$$N_{CVD} = \frac{k(T_s)h}{D(T_s)} \tag{118}$$

so as to yield

$$\frac{\partial C(x, p)}{\partial p}\bigg|_{p=0} = N_{CVD} C(x, 0). \tag{119}$$

The separation of variables method ($C(x, p) = X(x)P(p)$) gives, as before (see §3.2.),

$$X(x) = \exp\left(-\lambda^2 \frac{D(T)}{v_0 h}\frac{x}{h}\right) \tag{120}$$

$$P(p) = \alpha \sin(\lambda p) + \beta \cos(\lambda p). \tag{121}$$

From boundary condition equation (19) it is obtained that

$$P(p) = \beta \cos[\lambda(1 - p)]. \tag{122}$$

The general solution then is

$$C(x, p) = C_0 \sum_{n=1}^{\infty} \beta_n \cos[\lambda_n(1 - p)] \exp\left(-\lambda_n^2 \frac{D(T)}{v_0 h}\frac{x}{h}\right). \tag{123}$$

The constant λ_n can be found using boundary condition equation (119):

$$\lambda_n \tan \lambda_n = N_{CVD}. \tag{124}$$

Boundary condition equation (17) yields

$$C_0 = C_0 \sum_{n=1}^{\infty} \beta_n \cos[\lambda_n(1-p)]. \tag{125}$$

For a range of values of N_{CVD} (0–∞) the λ_n and β_n can be found by the previously described least-squares fitting method (see §3.5). The growth rate $R(x)$ is now:

$$\frac{R(x)}{v_0 C_0} = \frac{k(T_s)}{v_0}\frac{C(x,0)}{C_0}$$
$$= \frac{k(T_s)}{v_0}\sum_{n=1}^{\infty}\beta_n \cos(\lambda_n)\exp\left(-\lambda_n^2 \frac{D(T)}{v_0 h}\frac{x}{h}\right)$$
$$= \frac{D(T_s)}{v_0 h} N_{CVD} \sum_{n=1}^{\infty}\beta_n \cos(\lambda_n)\exp\left(-\lambda_n^2 \frac{D(T)}{v_0 h}\frac{x}{h}\right). \tag{126}$$

The two limiting cases (1) $N_{CVD} = 0$ and (2) $N_{CVD} = \infty$ yield an exponential factor of $(k(T_s)/v_0)(x/h)$ and $\frac{1}{4}\pi^2$ $(D(T_s)/v_0 h)(x/h)$ (first term), respectively, which was to be expected (cf model 7 and 1)). The transition from kinetically to diffusion-controlled growth occurs at $N_{CVD} = \pi^2/4$, which is easily calculated by equating the exponential factors in the two limiting cases and using the definition of the CVD number. In figure 11 the exponential factor λ_1^2 is shown as a function of N_{CVD}. It follows that for $N_{CVD} > \frac{1}{4}\pi^2$ the growth is diffusion controlled (thus independent of N_{CVD}), whereas for $N_{CVD} < \frac{1}{4}\pi^2$ the growth is controlled by surface kinetics (N_{CVD} dependency). Figure 12 shows the N_{CVD} dependency of the total deposition check parameter ω_n for $n = 1$, 5 and 10. It follows that for $N_{CVD} > \frac{1}{4}\pi^2$ the growth is diffusion controlled (one term is not enough to describe the growth), whereas for $N_{CVD} < \frac{1}{4}\pi^2$ the growth is controlled by surface kinetics (one term only ($n = 1$) is sufficient).

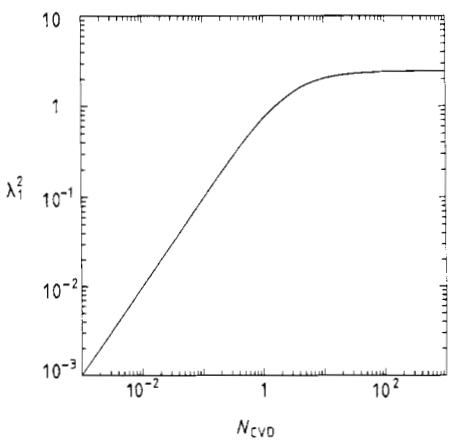

Figure 11. Exponential factor λ_1^2 as a function of N_{CVD}. Note that for $N_{CVD} > \frac{1}{4}\pi^2$ the growth is diffusion controlled (thus independent of N_{CVD}), whereas for $N_{CVD} < \frac{1}{4}\pi^2$ the growth is controlled by a reaction limited by surface kinetics (N_{CVD} dependency).

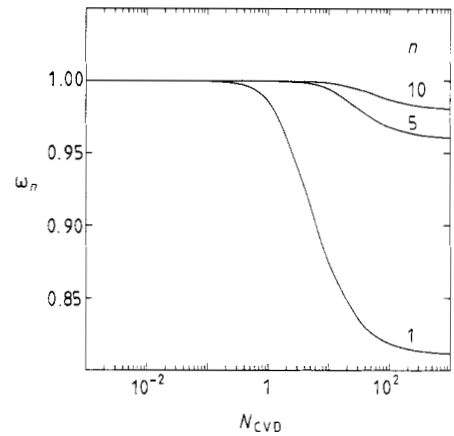

Figure 12. Total deposition parameter ω_n as a function of N_{CVD} for $n = 1$, 5 and 10. Note that for $N_{CVD} > \frac{1}{4}\pi^2$ the growth is diffusion controlled (more terms are needed to describe the growth), whereas for $N_{CVD} < \frac{1}{4}\pi^2$ the growth is controlled by a reaction limited by surface kinetics (one term only ($n = 1$) is sufficient).

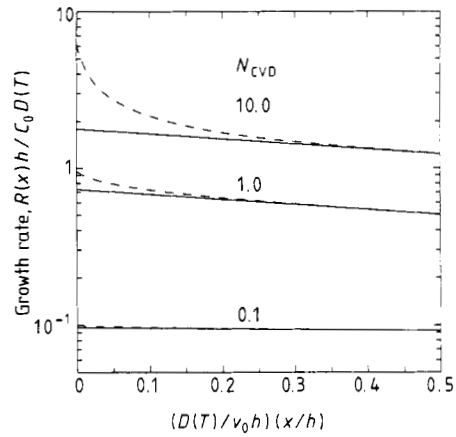

Figure 13. $R(x)h/C_0D(T)$ as a function of $(D(T)/v_0h)$ (x/h) for $N_{CVD} = 0.1$, 1.0 and 10.0 using $n = 1$ (full curves) and $n = 10$ (broken curves). Note that higher N_{CVD} increases the growth rate, but at the same time the depletion is stronger.

In figure 13 the growth rate $R(x)h/C_0D(T)$ is plotted as a function of $(D(T)/v_0h)(x/h)$ for three values of N_{CVD}, i.e. 0.1, 1.0 and 10. For small N_{CVD} no depletion occurs, but the growth rate is small. Higher N_{CVD} yields a higher growth rate, but also an increased depletion effect.

5. Conclusion

It is found that for all models an expression for the growth rate can be derived, which is a summation over a number of terms. The first term contributes in nearly all cases more than 90% to the complete expression. Therefore the growth rate can be described—in good approximation—by

$$R(x) = A\frac{D(T)}{v_0 h}\exp\left(-B\frac{D(T)}{v_0 h}\frac{x}{h}\right) \tag{127}$$

where the constants A and B are determined by the velocity profile used. Because of the correspondence of the results obtained for the concentration profile and growth rate between model 1 (plug flow) and model 6 (parabolic profile) the plug-flow profile may be used in the calculation of the concentration profile and growth rate in future models [16–18]. A model in which growth limited by surface kinetics (model 7) and diffusion-controlled growth (model 1, plug flow) are combined is derived (model 8) using CVD number N_{CVD}. In the limiting cases (1) $N_{CVD} = 0$ and (2) $N_{CVD} = \infty$ this model converges to model 7 and model 1, respectively, with a cross-over point at $N_{CVD} \sim \frac{1}{4}\pi^2$. In a forthcoming paper [16] a temperature gradient will be introduced and the effect of thermodiffusion will be studied. The derived models will then be applied to the growth of Si [17], GaAs [17, 18] and AlGaAs [18] and confronted with experimental growth results as found in e.g. [14].

Acknowledgments

This work was performed as a part of the research programme of the Netherlands Technology Foundation (STW) with financial support from the Netherlands Organisation for Scientific Research (NWO) and by the EC research contract no EN3S-0078-NL.

Appendix 1. Effect of deposition on reactor side walls

All the models treated so far are based on the assumption that the reactor is of infinite width (assumption 9), so as to reduce the problem to a two-dimensional one. This assumption has been made plausible above (§2.1) in the sense that only a small error is made using the assumption. This appendix treats the effect of the presence of reactor side walls using model 1 (isothermal, diffusion-controlled growth, plug flow). Two cases can be distinguished: (i) no deposition occurs upon the side walls and (ii) deposition does occur upon the side walls. In both cases the following partial differential equation has to be solved:

$$v_0 \frac{\partial C(x, y, z)}{\partial x} = D(T)\left(\frac{\partial^2 C(x, y, z)}{\partial y^2} + \frac{\partial^2 C(x, y, z)}{\partial z^2}\right). \tag{A1.1}$$

The two cases can be distinguished in terms of their boundary conditions.

A.1.1. No deposition upon side walls

If no deposition occurs upon the side walls, the following boundary conditions are valid:

$$C(x, 0, z) = 0 \qquad \text{(cf equation (18))} \tag{A1.2}$$

$$\left.\frac{\partial C(x, y, z)}{\partial y}\right|_{y=h} = 0 \qquad \text{(cf equation (19))} \tag{A1.3}$$

$$\left.\frac{\partial C(x, y, z)}{\partial z}\right|_{z=0} = 0 \tag{A1.4}$$

$$\left.\frac{\partial C(x, y, z)}{\partial z}\right|_{z=b} = 0 \tag{A1.5}$$

$$C(0, y, z) = C_0 \qquad \text{(cf equation (17))}. \tag{A1.6}$$

The method of solving equation (A1.1) is analogous to the one that is used for model 1 (see §3.2). Introducing the coordinate p ($p = D(T)x/v_0$) and using the separation of variables method ($C(x, y, z) = P(p)Y(y)Z(z)$) one obtains:

$$\frac{1}{P(p)}\frac{dP(p)}{dp} = \frac{1}{Y(y)}\frac{d^2Y(y)}{dy^2} + \frac{1}{Z(z)}\frac{d^2Z(z)}{dz^2} = -\lambda^2. \tag{A1.7}$$

Solving the left-hand term yields:

$$P(p) = \exp(-\lambda^2 p). \tag{A1.8}$$

Rearranging the right-hand term and equating it to a new constant ($-\mu^2$) results in the following partial differential equation to be solved:

$$\frac{1}{Y(y)}\frac{d^2Y(y)}{dy^2} = -\lambda^2 - \frac{1}{Z(z)}\frac{d^2Z(z)}{dz^2} = -\mu^2. \tag{A1.9}$$

The solution is:

$$Y(y) = \alpha \sin(\mu y) + \beta \cos(\mu y) \tag{A1.10}$$

$$Z(z) = \gamma \sin(\Phi z) + \delta \cos(\Phi z) \tag{A1.11}$$

with $\nu = -(\lambda^2 - \mu^2)$. From the boundary conditions equations (A1.2)-(A1.5) it is obtained that

$$\beta = 0 \qquad \mu = \frac{2n-1}{2}\frac{\pi}{h} \qquad n = 1, 2, 3 \ldots$$

$$\gamma = 0 \qquad \nu = m\frac{\pi}{b} \qquad m = 0, 1, 2 \ldots .$$

The complete solution then is obtained by summing all separate solutions, yielding:

$$C(x, y, z) = C_0 \sum_{m=0}^{\infty}\sum_{n=1}^{\infty} \alpha_{m,n} \sin\left(\frac{2n-1}{2}\pi\frac{y}{h}\right)\cos\left(m\pi\frac{z}{b}\right) \times \exp\left\{-\left[m^2\pi^2\left(\frac{h}{b}\right)^2 + \frac{(2n-1)^2\pi^2}{4}\right]\frac{D(T)}{v_0 h}\frac{x}{h}\right\}. \tag{A1.13}$$

The factor $\alpha_{m,n}$ is determined using boundary condition equation (A1.6) and a double Fourier transformation; this gives

$$\alpha_{m,n} = \frac{8}{(2n-1)b\pi}\int_0^b \cos\left(m\pi\frac{z}{b}\right)dz \qquad m = 1, 2, 3, \ldots$$

$$\alpha_{0,n} = \frac{4}{(2n-1)b\pi}\int_0^b dz. \tag{A1.14}$$

It follows that $\alpha_{m,n} = 0$ for all $m \neq 0$, hence the expression for the growth rate is exactly the same as derived

previously for model 1 (equation (27)):

$$\frac{R(x)}{v_0 C_0} = 2\frac{D(T)}{v_0 h}\sum_{n=1}^{\infty}\exp\left(-\frac{(2n-1)^2\pi^2}{4}\frac{D(T)}{v_0 h}\frac{x}{h}\right). \tag{A1.15}$$

The conclusion is that the growth rate is independent of the z coordinate in the case that no deposition occurs at the side walls, which was made plausible above in §2.1 (see figure 3).

A.1.2. Deposition upon side walls

In the case of deposition upon the side walls the derivation goes analogous to the previous one in §A.1.1. However, boundary conditions equations (A1.4) and (A1.5) must be replaced by:

$$C(x, y, 0) = 0 \tag{A1.16}$$

$$C(x, y, b) = 0. \tag{A1.17}$$

It should be remarked that it is assumed that the deposition upon the side walls is the same as on the susceptor. This will not be true in practice, because of the strong temperature gradient in the gas phase, which results in a strong temperature gradient that exists at the side walls in the y direction. The result of the derivation is:

$$C(x, y, z) = C_0\sum_{m=1}^{\infty}\sum_{n=1}^{\infty}\alpha_{m,n}\sin\left(\frac{2n-1}{2}\pi\frac{y}{h}\right)\sin\left(m\pi\frac{z}{b}\right) \times \exp\left\{-\left[m^2\pi^2\left(\frac{h}{b}\right)^2 + \frac{(2n-1)^2\pi^2}{4}\right]\frac{D(T)}{v_0 h}\frac{x}{h}\right\} \tag{A1.18}$$

with

$$\alpha_{m,n} = \frac{16}{(2n-1)m\pi^2} \qquad m \text{ odd} \tag{A1.19}$$

$$\alpha_{m,n} = 0 \qquad m \text{ even}.$$

Using a new summation parameter k ($m = 2k - 1$) the growth rate can be written as:

$$\frac{R(x, z)}{v_0 C_0} = \frac{8}{\pi}\frac{D(T)}{v_0 h}\sum_{k=1}^{\infty}\sum_{n=1}^{\infty}\frac{1}{2k-1}\sin\left((2k-1)\pi\frac{z}{b}\right) \times \exp\left\{-\left[(2k-1)^2\pi^2\left(\frac{h}{b}\right)^2 + \frac{(2n-1)^2\pi^2}{4}\right]\frac{D(T)}{v_0 h}\frac{x}{h}\right\}. \tag{A1.20}$$

The growth rate can be rewritten as a product of two functions $f(s, t)$ and $g(x)$:

$$\frac{R(x, z)}{v_0 C_0} = f(s, t)g(x) \tag{A1.21}$$

$$f(s, t) = \frac{4}{\pi}\sum_{k=1}^{\infty}\frac{1}{2k-1}\sin[(2k-1)\pi s] \times \exp[-(2k-1)^2\pi^2 t] \tag{A1.22}$$

$$g(x) = 2\frac{D(T)}{v_0 h}\sum_{n=1}^{\infty}\exp\left[-\frac{(2n-1)^2\pi^2}{4}\frac{D(T)}{v_0 h}\frac{x}{h}\right] \tag{A1.23}$$

with

$$s = \frac{z}{b} \qquad t = \frac{D(T)}{v_0 h}\frac{x}{h}\left(\frac{h}{b}\right)^2. \tag{A1.24}$$

The function $g(x)$ is equal to the expression for the growth rate if no deposition occurs at the side walls (equation (27) in §3.2 and equation (A.15) in §A.1.1). The dimensionless functions $f(s, t)$ varies between 1 and 0 and can be seen as a correction to $g(x)$. For $t = 0$ ($x = 0$ or $b \to \infty$) $f(s, t)$ reaches its maximum (1) and is independent of s. In figures 14 and 15 the correction function $f(s, t)$ is depicted as function of the lateral (s) and axial (t) position, respectively. It appears that the correction function $f(s, t)$ is independent of the height h of the reactor, whereas the surface on to which crystal growth occurs (i.e. the side walls) does depend on h. The width b of the reactor has a strong influence on $f(s, t)$. For sufficiently small values of t it follows that there exists a region in the middle of the reactor where $f(s, t)$ is nearly independent of s. In table 11 some values of s and t are listed for which $f(s, t)$ equals 0.99 and 0.9, respectively.

Although the expression for the growth rate with the correction function $f(s, t)$ has been derived for a relatively simple model (isothermal, diffusion-controlled growth, plug flow), it is expected that also for more complex models the growth rate can be described as a product of a growth rate and a correction function similar to $f(s, t)$. Therefore it is concluded that the growth rate is nearly independent of the z coordinate in the case that deposition occurs at the side walls (see §2.1).

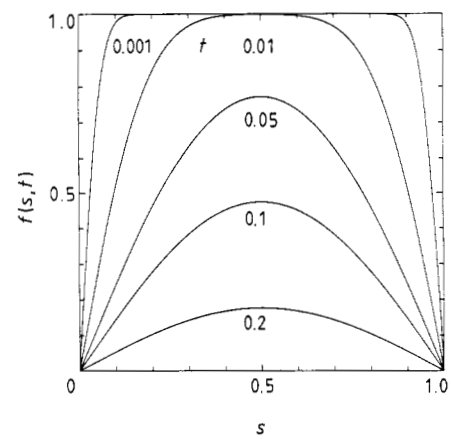

Figure 14. The dimensionless correction function $f(s, t)$ as a function of lateral (s) position.

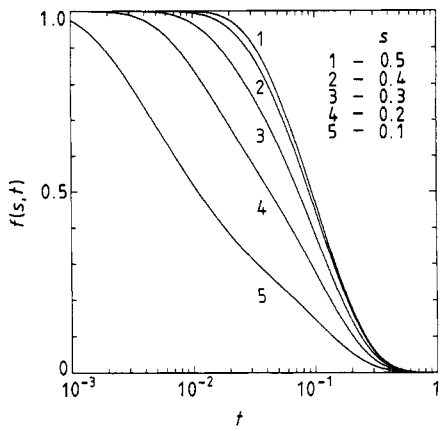

Figure 15. The dimensionless correct function $f(s, t)$ as a function of axial (t) position.

Table 11. Boundary values for $f(s, t)$

	t	
s	$f(s, t) = 0.99$	$f(s, t) = 0.9$
0.5	0.0158	0.0325
0.4	0.0120	0.0276
0.3	0.0067	0.0166
0.2	0.0030	0.0074
0.1	0.0001	0.0018

Appendix 2. Effect of axial diffusion

To study the influence of diffusion of growth components in the axial direction (x) model 1 (isothermal, diffusion-controlled growth, plug flow) is used. The following partial differential equation has to be solved:

$$v_0 \frac{\partial C(x, y, z)}{\partial x} = D(T)\left(\frac{\partial^2 C(x, y, z)}{\partial x^2} + \frac{\partial^2 C(x, y, z)}{\partial y^2}\right). \tag{A2.1}$$

The boundary conditions are the same as in §3.2, i.e. equations (17)–(19). Separation of variables ($C(x, y) = X(x)Y(y)$) yields

$$\frac{v_0}{D(T)}\frac{1}{X(x)}\frac{\mathrm{d}X(x)}{\mathrm{d}x} - \frac{1}{X(x)}\frac{\mathrm{d}^2X(x)}{\mathrm{d}x^2} = \frac{1}{Y(y)}\frac{\mathrm{d}^2Y(y)}{\mathrm{d}y^2} = -\lambda^2. \tag{A2.2}$$

Analogous to §3.2 (equation (22)) solution of the right-hand term gives

$$Y(y) = \alpha \sin(\lambda y) + \beta \cos(\lambda y) \tag{A2.3}$$

with

$$\beta = 0 \qquad \lambda = \frac{2n-1}{2}\frac{\pi}{h} \qquad \text{with } n = 1, 2, 3 \ldots.$$

The solution of the left-hand term is

$$X(x) = \gamma \exp(-\mu_+ x) + \delta \exp(-\mu_- x) \tag{A2.4}$$

with

$$\mu_\pm = \frac{v_0}{2D(T)} \pm \sqrt{\left(\frac{v_0}{2D(T)}\right)^2 + \lambda^2}.$$

It follows that $\gamma = 0$, because $\mu > 0$ is physically not valid. Therefore the growth rate can be expressed as

$$\frac{R(x)}{v_0 C_0} = 2\frac{D(T)}{v_0 h}\sum_{n=1}^{\infty}\exp\left[\frac{1}{2}\left(\frac{v_0 h}{D(T)} - \sqrt{\left(\frac{v_0 h}{D(T)}\right)^2 + (2n-1)^2\pi^2}\right)\frac{x}{h}\right]. \tag{A2.5}$$

The square root can be approximated with the first term of its Taylor expansion, if

$$\frac{v_0 h}{D(T)} \gg (2n-1)\pi. \tag{A2.6}$$

Under this condition equation (A2.5) equals the expression for the growth rate as derived in §3.2 (equation (27)), however, this condition cannot always be met. The exact ratio $r(x)$ of the growth rate without and with axial diffusion, respectively, is given by

$$r(x) = \frac{R_{\text{without}}(x)}{R_{\text{with}}(x)} = \frac{\sum_{n=1}^{\infty}\exp\left[-\frac{(2n-1)^2}{4}\pi^2 t\right]}{\sum_{n=1}^{\infty}\exp\left[\frac{s}{2}\left(1 - \sqrt{1 + (2n-1)^2\pi^2\frac{t}{s}}\right)\right]} \tag{A2.7}$$

with

$$s = \frac{v_0 h}{D(T)}\frac{x}{h} \qquad t = \frac{D(T)}{v_0 h}\frac{x}{h}. \tag{A2.8}$$

The ratio $r(x)$ is shown in figure 16. For small t the ratio $r(x)$ is nearly independent of t and $r(x)$ reaches 1 fast with increasing s. For large t the ratio $r(x)$ depends strongly on t and decreases fast to 0. It should be noted that s and t are coupled variables through $D(T)$, v_0 and x. Effects related to axial diffusion may safely be neglected in cases where $s > 30$ and $t < 1$. In a reactor with $h = 2$ cm and

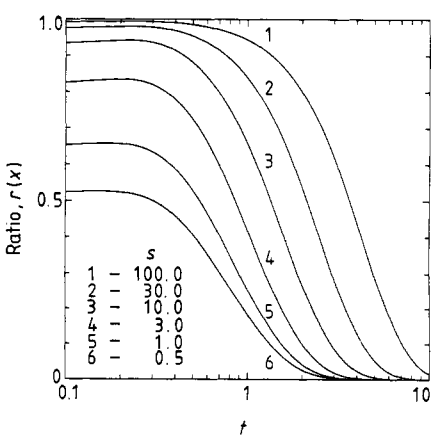

Figure 16. The ratio $r(x)$ indicating the importance of axial diffusion as a function of t with s as parameter.

$T = 700$ °C we typically use $v_0 = 10$ cm s^{-1}, which must be corrected to roughly twice its value [16]. With $D(T) = D_0(T/T_0)^{1.7}$ and $D_0 = 0.6$ cm^2 s^{-1} (TMG) [28] we then arrive at $r(x) = 0.97$ for $x = 8$ cm and $r(x) = 0.95$ for $x = 16$ cm. A velocity v_0 of 5 cm s^{-1} results in $r(x) = 0.92$ and 0.83 for $x = 8$ and 16 cm, respectively. Therefore it appears that the effect of axial diffusion becomes stronger towards the end of the susceptor, which is to be expected as the axial diffusion term in equation (A2.1) increases with x.

The corrected expression for the growth rate has been derived for a relatively simple model (isothermal, diffusion-controlled growth, plug flow); it is nevertheless expected that the small deviations found are similar for more complex models. Therefore it is concluded that the growth rate is nearly independent of axial diffusion of the growth components, as is also concluded in [8], provided that a susceptor is used which is not too long.

References

[1] Ludowise M J 1985 *J. Appl. Phys.* **58** R3
[2] Kuech T F 1987 *Mater. Sci. Rep.* **2** 1
[3] Manasevit H M and Simpson W I 1969 *J. Electrochem. Soc.* **116** 1725
[4] van de Ven J, Rutten G M J, Raaijmakers M J and Giling L J 1986 *J. Cryst. Growth* **76** 352
[5] Coltrin M E, Kee R J and Miller J A 1984 *J. Electrochem. Soc.* **131** 425
[6] Fotiadis D I, Kremer A M, McKenna D R and Jensen K F 1987 *J. Cryst. Growth* **85** 154
[7] Moffat H K and Jensen K F 1986 *J. Cryst. Growth* **77** 108
[8] Ouazzani J, Chiu K-C and Rosenberger F 1988 *J. Cryst. Growth* **91** 497
[9] Rhee S, Szekely J and Ilegbusi O J 1987 *J. Electrochem. Soc.* **134** 2552
[10] Bird R B, Stewart W E and Lightfoot E N 1960 *Transport Phenomena* (New York: Wiley)
[11] Reep D H and Ghandhi S K 1983 *J. Electrochem. Soc.* **130** 675
[12] Dapkus P D, Manasevit H M, Hess K L, Low T S and Stillman G E 1981 *J. Cryst. Growth* **55** 10
[13] Escobosa A, Kraeutle H and Beneking H 1982 *J. Cryst. Growth* **57** 605
[14] van Sark W G J H M, Janssen G J H M, de Croon M H J M, Giling L J, Arnold Bik W M, Dunselman C P M, Habraken F H P M and van der Weg W F 1988 *J. Appl. Phys.* **64** 195
[15] Stringfellow G B and Hall H T 1978 *J. Cryst. Growth* **43** 47
[16] van Sark W G J H M, de Croon M H J M, Janssen G and Giling L J 1990 *Semicond. Sci. Technol.* **5** 36
[17] van Sark W G J H M, de Croon M H J M, Janssen G and Giling L J 1990 *Semicond. Sci. Technol.* **5** at press
[18] van Sark W G J H M, de Croon M H J M and Giling L J 1989 *J. Appl. Phys.* submitted for publication
[19] Giling L J 1985 *Crystal Growth of Electronic Materials* ed. E Kaldis (Amsterdam: Elsevier) p 71
[20] Visser E P, Govers C A M, Giling L J, Kleijn C R and Hoogendoorn C J 1989 *J. Cryst. Growth* **94** 929
[21] de Croon M H J M and Giling L J 1988 *J. Cryst. Growth* **93** 932
[22] de Croon M H J M and Giling L J 1989 *J. Electrochem. Soc.* submitted for publication
[23] *Handbook of Chemistry and Physics* 1978-9 ed. R C Weast 59th edn (Cleveland, OH: CRC) A-101
[24] Spiegel M R 1974 *Schaum's Outline of Theory and Problems of Fourier Analysis* (New York: McGraw-Hill)
[25] *Handbook of Mathematical Functions* 1972 ed. M Abramowitz and I A Stegun (New York: Dover)
[26] van den Brekel C H J 1977 *Philips Res. Rep.* **32** 118
[27] van den Brekel C H J and Bloem J 1977 *Philips Res. Rep.* **32** 134
[28] Suzuki M and Sato M 1985 *J. Electrochem. Soc.* **132** 1684

List of symbols

a,b	parameters in Kummer's function $M(a; b; z)$
a_v, b_v	parameters in $v(y)$ (model 5)
A_n, A_i, A, A'	pre-exponential factor in growth rate
b	width of reactor
B_n, B_i, B, B'	exponential factor in growth rate
c_p	specific heat
$C(x, y, z, t)$, $C(x, y)$, $C(x)$	concentration of growth species
$C_i(x, y, z, t)$	concentration of ith growth species
C_0	input concentration of the group III component
C_{tot}	total gas phase concentration
$D(T)$	binary diffusion coefficient of the group III component
D_0	binary diffusion coefficient at $T = T_0$
E_a	activation energy
$f(s, t)$	correction function of growth rate
F_k^2	minimalisation function
$g(x)$	growth rate
h	height of reactor
h_p	Planck constant
i	summation parameter
$J(x, y)$	diffusional flux
$J_n(x)$	Bessel function of first kind of order n
k	reaction rate of surface reaction, summation parameter
k_B	Boltzmann constant
m	summation parameter
$M(a; b; z)$	confluent hypergeometric function (Kummer)
n	summation parameter
$n(x, y, z, t)$	mole fraction of growth species
N_0	total amount of input growth species
N_{CVD}	dimensionless CVD number
p, p'	help coordinate
P	total pressure
$P(p)$	y-dependent part of $C(x, y)$
q	help coordinate

$r(x)$	ratio of growth rates
$R(x)$	growth rate
Re	Reynolds number
R_g	gas constant
s	help parameter
t	time, help parameter
T	temperature
$T(x, y, z, t)$, $T(y)$	temperature profile
T_0	temperature at top of reactor
T_s	substrate temperature
$v(x, y, z, t)$, $v(y)$	velocity profile
v_0	plug-flow velocity
$\bar{v}$	average velocity
x	axial coordinate
x_v	entrance length velocity profile
x_T	entrance length temperature profile
$X(x)$	x-dependent part of $C(x, y)$
y	vertical coordinate
$Y(y)$	y-dependent part of $C(x, y)$
$Y_1(q)$, $Y_2(q)$	y-dependent parts of $C(x, y)$
z	lateral coordinate
$Z(z)$	z-dependent part of $C(x, y, z)$
α, $\alpha_{m,n}$, α_n	help parameter, pre-exponential factor
α', α'_m, α'_n	help parameter, pre-exponential factor
α''_k, α''_n	pre-exponential factor
α_T	thermal diffusion factor
β	help parameter, pre-exponential factor, factor in temperature dependence of κ
β_n	pre-exponential factor
β', β'_m, β'_n	help parameter, pre-exponential factor
β'', β''_k	pre-exponential factor
γ	help parameter, factor in temperature dependence of $D(T)$
$\Gamma(x)$	gamma function
δ	help parameter, height (model 5)
κ	heat transfer coefficient
κ_0	heat transfer coefficient at $T = T_0$
λ, λ_m, λ_n	roots of equation
μ, μ_m, μ_n	roots of equation
μ_+, μ_-	roots of equation
ν, ν_k, ν_n	roots of equation
ρ	density of gas
ω, ω_∞	total deposition check parameter
ω_n, ω_1	total deposition check parameter, using n, 1 term(s)